


Article

Low Energy Cost Synchronization Strategy for Markovian Switching Complex Systems/Networks: Multiple Perspectives Comparative Analysis

Qian Xie ^{1,*} , Haolan Xu ¹, Jian Dang ¹ and Zhe Wang ²

¹ School of Electrical Engineering, Xi'an University of Technology, Xi'an 710048, China; xuhl0929@foxmail.com (H.X.); dangjian@xaut.edu.cn (J.D.)

² Institute of Water Resources and Hydro-Electric Engineering, Xi'an University of Technology, Xi'an 710048, China; wangzhewater@xaut.edu.cn

* Correspondence: xieq@xaut.edu.cn; Tel.: +86-153-9909-5450

Abstract: In this paper, the low energy cost synchronization control strategy of Markovian switching complex systems/networks is mainly studied and analyzed through multiple perspectives. Firstly, in order to achieve synchronization of Markovian switching complex networks with low energy cost, a control scheme based on the optimal node selection strategy that does not depend on the network coupling strength is improved, and a finite-time controller with a simpler structure is constructed. Secondly, based on the event-triggered control strategy an effective trigger event is designed to achieve the low energy cost synchronization of Markovian switching complex networks on the basis of reducing the information transmission and interaction between networks. Finally, the two control strategies mentioned in this paper are compared and analyzed from multiple perspectives through numerical simulations to better guide practical engineering.

Keywords: Markovian switching; complex systems/networks; pinning control strategy; event-triggered control strategy



Citation: Xie, Q.; Xu, H.; Dang, J.; Wang, Z. Low Energy Cost Synchronization Strategy for Markovian Switching Complex Systems/Networks: Multiple Perspectives Comparative Analysis. *Processes* **2024**, *12*, 232. <https://doi.org/10.3390/pr12010232>

Academic Editor: Jie Zhang

Received: 3 January 2024

Revised: 17 January 2024

Accepted: 18 January 2024

Published: 21 January 2024



Copyright: © 2024 by the authors. Licensee MDPI, Basel, Switzerland. This article is an open access article distributed under the terms and conditions of the Creative Commons Attribution (CC BY) license (<https://creativecommons.org/licenses/by/4.0/>).

1. Introduction

Complex systems and networks have received increasing recognition as an important tool for portraying and understanding real systems, especially in various fields such as biology, social systems, and engineering technology. Real systems often suffer from unexpected situations during operation, such as sudden changes in the environment, connection failure of the system, and system failure or maintenance, etc. [1–3]. These unexpected situations may cause the network topology to be re-linked, and thus the network operation state will be changed. The Markovian switching process can accurately describe such system/network topology switching process, and the system/network can be switched from one mode to another by Markov Process, which also coincides with the topology changes of the system/network [4–6]. Therefore, the complex network model with Markovian switching process gradually attracts the attention of many scholars and becomes a hot topic of current research.

Synchronization is an important class of clustering phenomena among the many dynamical behaviors of Markovian switching complex networks and has received more attention [7]. With the increasing standard of practical engineering requirements, the synchronization performance of the network is no longer the only criterion to measure network synchronization, as low control cost and low energy loss have become another concern of practical engineering. The commonly used control strategies are pinning control [8], linear (nonlinear) feedback control [9], adaptive control [10], intermittent control [11], impulse control [12], event-triggered control [13], etc. The characteristics of low energy consumption and low control cost of pinning control and event-triggered control have attracted the

attention of many scholars. This paper will analyze the low-energy synchronous control problem of Markovian switching complex networks from multiple perspectives (optimal node selection strategy and event-triggered control strategy), to provide some theoretical basis for practical engineering.

It is well known that the pinning control strategy mainly reduces the control cost of the network on the basis of achieving synchronization by controlling a small number of nodes. However, how to select the control nodes of the network has been the focus of pinning control strategy research. In order to achieve the synchronization of the proposed multi-weight network model, an effective pinning controller was proposed in Ref. [14]. Same as Ref. [14], Ref. [15] only aims to achieve the synchronization behavior of the network by designing an effective and reliable pinning controller, but the importance of network pinning nodes selection is ignored. The problem of controlled node selection for pinning control strategy has been considered in Refs. [16–18], and the authors have proposed effective controlled node selection schemes while using pinning control strategies. However, during the Markovian switching complex network synchronization process, the performance metrics of each node in the network are dynamically changing, and how to track and exert control over these important nodes at each moment must also be considered. Moreover, the event-triggered control strategy reduces the information transmission and interaction between networks mainly through the designed trigger function, thus reducing the cost and energy loss of network control while achieving network synchronization [19,20]. Therefore, this paper will establish a node performance measure to track and control the important nodes at each moment, thereby achieving network synchronization with low energy consumption and low control cost, and better guide practical engineering.

Based on the above discussion, this paper mainly analyzes the pinning control (optimal node selection strategy) and event-triggered control strategy through multiple perspectives, and studies how to synchronize the network with low energy cost and low control cost, so as to better provide a theoretical basis for practical engineering. To the best of the knowledge of the authors, there are few studies on the node selection problem of pinning control strategy, and there is currently no comparative study on optimal node selection strategy and event-triggered control strategy. Therefore, this research has certain theoretical and practical value.

This paper aims to achieve Markovian Switching complex network synchronization under low energy control cost and gives the basis for using the optimal node selection strategy and event-triggered control strategy under different actual conditions. For weakly coupling strength medium scale networks, the optimal node selection strategy can control less nodes to achieve faster low energy cost synchronization. For large scale networks with strong coupling strength, the event-triggered control strategy can achieve low energy cost synchronization faster, but requires slightly more nodes to be controlled than the optimal node selection strategy.

The rest of this paper is organized as follows. Some necessary formulas and mathematical models of network are given in Section 2. In Section 3, the control scheme based on the optimal node selection strategy is improved, and a controller with a simpler structure is constructed to achieve network synchronization with low control cost and low energy consumption. The theoretical proof of finite-time synchronization is given via the event-triggered control strategy in Section 4. In Section 5, the advantages and disadvantages of the two control methods are discussed through numerical simulations, and some conclusions are drawn for practical engineering purposes. Finally, Section 6 concludes the paper.

2. Network Models and Mathematical Preliminaries

In this section, some necessary assumptions and lemmas are given to complete the theoretical proof of Sections 3 and 4.

We define a right-continuous Markovian process $\{r(t), t \geq 0\}$ in the complete probability space $(\Omega, F, \{F_t\}_{t \geq 0}, P)$, which takes values in the finite state space $C = \{1, 2, \dots, m\}$ with

generator $\Pi = (\pi_{pq})_{m \times m}$ ($p, q \in C$). Define the transition probability (from the p -th mode at time t to the q -th mode at time $t + \Delta t$) in the following form:

$$P\{r(t + \Delta t) = q | r(t) = p\} = \begin{cases} \pi_{pq}\Delta t + o(\Delta t) & \text{if } q \neq p \\ 1 + \pi_{pp}\Delta t + o(\Delta t) & \text{if } q = p \end{cases} \quad (1)$$

where $\lim_{\Delta t \rightarrow 0} \frac{o(\Delta t)}{\Delta t} = 0$ ($\Delta t > 0$), and $\pi_{pq} \geq 0$ is the transition rate that satisfies:

$$\pi_{pp} = - \sum_{q=1, q \neq p}^m \pi_{pq} \quad (2)$$

Consider a multiple weights Markovian switching complex dynamical network composed of N nodes with stochastic perturbations, in which each node is an n -dimensional dynamical system.

$$\begin{aligned} \dot{x}_i(t) = & f(t, x_i(t)) + c_1 \sum_{j=1}^N a_{ij}(r(t))\Gamma_1 x_j(t) + c_2 \sum_{j=1}^N b_{ij}(r(t))\Gamma_2 x_j(t) \\ & + \sigma_i(t, x_i(t), r(t))\dot{\omega}(t), \quad i = 1, 2, \dots, N. \end{aligned} \quad (3)$$

where $x_i(t) = (x_{i1}(t), x_{i2}(t), \dots, x_{in}(t))^T \in R^n$ is the state vector of node i ; $f: R^n \rightarrow R^n$ is a nonlinear vector function on $x(t)$; $c_1, c_2 > 0$ denote the coupling strength of the network. Here, $\Gamma_1 \in R^{n \times n}$ and $\Gamma_2 \in R^{n \times n}$ are inner coupling matrices. $A(r(t)) = (a_{ij}(r(t)))^{N \times N} \in R^{N \times N}$ and $B(r(t)) = (b_{ij}(r(t)))^{N \times N} \in R^{N \times N}$ are the matrices representing the topological structure of the network at time t of mode $r(t)$. $\omega(t) = (\omega_1(t), \omega_2(t), \dots, \omega_n(t))^T$ is an n -dimensional Brown motion; $\sigma_i(t, x_i(t), r(t))$ is the noisy intensity function, mainly used to describe the interference brought by the actual environment to the system.

The uncoupled node of the network (3) is given by:

$$\dot{s}(t) = f(t, s(t)) \quad (4)$$

Here, the uncoupled node $s(t)$ can be regarded as an isolated node system of the network (3).

Then, some lemmas and assumptions are given as follow.

Lemma 1 [21]. Assume that b_1, b_2, \dots, b_n are positive numbers, and c ($0 < c < 1$) is a positive constant. Then the following inequality holds

$$(b_1 + b_2 + \dots + b_n)^c \leq b_1^c + b_2^c + \dots + b_n^c \quad (5)$$

Assumption 1. There exists a non-negative constant ν and a symmetric positive matrix P , for $\forall x(t), y(t) \in R^n$, the nonlinear function $f(\cdot)$ satisfies

$$(x(t) - y(t))^T (f(t, x(t)) - f(t, y(t))) \leq (x(t) - y(t))^T \nu P (x(t) - y(t)) \quad (6)$$

Assumption 2. There exists a non-negative constant ρ_i , and the noise intensity function $\sigma_i(t, e_i(t), r(t))$ satisfies the uniform Lipschitz condition, such that

$$\text{trace} \left[\sigma_i^T(t, e_i(t), r(t)) \sigma_i(t, e_i(t), r(t)) \right] \leq \rho_i(r(t)) e_i^T(t) e_i(t) \quad (7)$$

3. Finite-Time Synchronization of Markovian Switching Complex Networks with Low Control Cost and Low Energy Consumption Based on Optimal Nodes Control Strategy

Based on the optimal node control strategy proposed in the previous research of the authors [22], combined with the Markovian switching complex network characteristics, sorting according to the node importance measurement indicators at different time intervals, some important nodes (nodes with greater impact on system synchronization) are selected as controlled nodes, and we then establish network models at different time intervals and design a controller with a simpler structure to achieve synchronization with low control cost and low energy consumption.

The Markovian switching complex network model based on the optimal node selection strategy in the time interval $(t_{k-1}, t_k]$ can be written as

$$\begin{cases} \dot{x}_i^k(t) = f(t, x_i^k(t)) + c_1 \sum_{j=1}^N a_{ij}(r(t)) \Gamma_1 x_j^k(t) + c_2 \sum_{j=1}^N b_{ij}(r(t)) \Gamma_2 x_j^k(t) \\ \quad + \sigma_i^k(t, x_i^k(t), r(t)) \dot{\omega}(t) + u_i^k(t), \quad i = o_{\max}^k(1), o_{\max}^k(2), \dots, o_{\max}^k(l^k) \\ \dot{x}_i^k(t) = f(t, x_i^k(t)) + c_1 \sum_{j=1}^N a_{ij}(r(t)) \Gamma_1 x_j^k(t) + c_2 \sum_{j=1}^N b_{ij}(r(t)) \Gamma_2 x_j^k(t) \\ \quad + \sigma_i^k(t, x_i^k(t), r(t)) \dot{\omega}(t), \quad \text{other} \end{cases} \quad (8)$$

where $o_{\max}^k(\iota), \iota = 1, 2, \dots, l^k$ denote the number of control nodes; $x_i^k(t)$ and $u_i^k(t)$ are the state variables and controller at time t_k .

According to Equations (4) and (8), the state error equation of the i -th node in network at time t_k is described as

$$e_i^k(t) = x_i^k(t) - s(t), \quad i = 1, 2, \dots, N. \quad (9)$$

We then bring (9) into (8), and the synchronization error dynamics system in the time interval $(t_{k-1}, t_k]$ can be obtained

$$\begin{cases} \dot{e}_i^k(t) = f(t, x_i^k(t)) - f(t, s(t)) + c_1 \sum_{j=1}^N a_{ij}(r(t)) \Gamma_1 e_j^k + c_2 \sum_{j=1}^N b_{ij}(r(t)) \Gamma_2 e_j^k \\ \quad + \sigma_i^k(t, e_i^k(t), r(t)) \dot{\omega}(t) + u_i^k, \quad i = o_{\max}^k(1), o_{\max}^k(2), \dots, o_{\max}^k(l^k) \\ \dot{e}_i^k(t) = f(t, x_i^k(t)) - f(t, s(t)) + c_1 \sum_{j=1}^N a_{ij}(r(t)) \Gamma_1 e_j^k + c_2 \sum_{j=1}^N b_{ij}(r(t)) \Gamma_2 e_j^k \\ \quad + \sigma_i^k(t, e_i^k(t), r(t)) \dot{\omega}(t), \quad \text{other} \end{cases} \quad (10)$$

Obviously, as the above formula is the error system in the time interval $(t_{k-1}, t_k]$, then only when the error system (9) converges to zero in a finite time interval $k = 1, 2, \dots, \Delta (\Delta \rightarrow \infty)$, can the network (3) achieve finite-time synchronization through the optimal node selection strategy. Therefore, it is particularly important to design an efficient controller based on the optimal node selection strategy.

Theorem 1. *Based on optimal node selection strategy, the following controller is designed.*

$$\begin{cases} u_i^k(t) = -\eta_i(r(t)) e_i^k(t) - \varphi(r(t)) \text{sign}(e_i^k(t)) |e_i^k(t)|^k, \quad \text{if } e_i^k(t) \neq 0 \\ u_i^k(t) = 0, \quad \text{if } e_i^k(t) = 0 \\ i = o_{\max}^k(1), o_{\max}^k(2), \dots, o_{\max}^k(l^k), k = 1, 2, \dots, \Delta \end{cases} \quad (11)$$

where $\text{sign}(e_i^k(t)) = \text{diag}\{\text{sign}(e_{i1}^k(t)), \text{sign}(e_{i2}^k(t)), \dots, \text{sign}(e_{in}^k(t))\}$; $\eta_i(r(t))$ and $\varphi(r(t))$ are positive constants, $r \in \mathcal{C}$. If the following inequalities are formed

$$\begin{cases} \Omega + \Lambda + \hat{A} + \hat{B} + \left(\frac{1}{2}\Theta(r(t)) - \Xi(r(t))\right) \otimes I_N \leq 0 \\ \sum_{q=1}^m \pi_{pq}(D(q) - Q(p)) \leq 0 \end{cases} \quad (12)$$

where $\hat{A}(r) = c_1 \frac{\tilde{A}(r)\tilde{A}^T(r)}{2}$, $\tilde{A}(r) = A(r) \otimes \Gamma_1$; $\hat{B}(r) = c_2 \frac{\tilde{B}(r)\tilde{B}^T(r)}{2}$, $\tilde{B}(r) = B(r) \otimes \Gamma_2$; $\Theta(r(t)) = \text{diag}\{\underbrace{\rho_1(r(t)), \dots, \rho_{o_{\max}(l_k)}(r(t))}_{l^k}, \underbrace{0, \dots, 0}_{N-l^k}\}$; $\Xi(r(t)) = \text{diag}\{\underbrace{\eta_1(r(t)), \dots, \eta_{o_{\max}(l_k)}(r(t))}_{l^k}, \underbrace{0, \dots, 0}_{N-l^k}\}$; $\Omega = \nu I_N \otimes P$; $\Lambda = I_N \otimes v_p$, $v_p = \sum_{q=1}^m \frac{1}{2} \pi_{pq}(D(q) - Q(p))$, $D(q)$ is an appropriate positive definite matrix, $Q(p)$ is any symmetrical matrix; I is an identity matrix; $I_N = \text{diag}\{\underbrace{1, \dots, 1}_{l^k}, \underbrace{0, \dots, 0}_{N-l^k}\}$. Thus, the synchronization of (3) can be achieved within a finite time t^* .

$$t^* \leq \frac{V(0, e(0), r(0))^{1-\gamma}}{\mu 2^\gamma (1-\gamma)} \quad (13)$$

where $\sigma = \min(\varphi(r(t)))$; $\gamma = (1 + \beta)/2$; $\mu = \varrho \min(\sigma, \lambda/2^{(1+\beta)/2}, 1)$, ϱ is an appropriate positive constant; $V(0, e(0), r(0)) = \frac{1}{2} \sum_{i=1}^N e_i^T(0) e_i(0)$; $e_i(0)$ is the initial condition.

Proof. In the time interval $(t_{k-1}, t_k]$, the following Lyapunov function is constructed:

$$V^k(t, e^k(t), p) = \frac{1}{2} \sum_{i=1}^N (e_i^k(t))^T e_i^k(t) \quad (14)$$

According to the differential operator L [23], the above Lyapunov function can be written as

$$\begin{aligned} \mathcal{L}V^k(t, e^k(t), p) &= \sum_{i=1}^N (e_i^k(t))^T \dot{e}_i^k(t) + \sum_{q=1}^m \pi_{pq} \frac{1}{2} \sum_{i=1}^N (e_i^k(t))^T e_i^k(t) \\ &+ \frac{1}{2} \sum_{i=1}^N [\text{trace}(\sigma_i^k(t, e_i^k(t), p))]^T \sigma_i^k(t, e_i^k(t), p) \end{aligned} \quad (15)$$

Bringing the error system (10) and the controller (11) into the above equation, we have

$$\begin{aligned} \mathcal{L}V^k(t, e^k(t), p) &= \sum_{i=1}^N (e_i^k(t))^T \left\{ f(t, x_i^k(t)) - f(t, s(t)) - \varphi(r(t)) \text{sign}(e_i^k(t)) |e_i^k(t)|^k \right. \\ &\quad \left. - \eta_i(r(t)) e_i^k(t) + c_1 \sum_{j=1}^N a_{ij}(p) \Gamma_1 e_j^k(t) + c_2 \sum_{j=1}^N b_{ij}(p) \Gamma_2 e_j^k(t) \right\} \\ &+ \frac{1}{2} \sum_{i=1}^N \left[\text{trace}(\sigma_i^k(t, e_i^k(t), p))]^T \sigma_i^k(t, e_i^k(t), p) \right] \\ &+ \sum_{q=1}^m \pi_{pq} \frac{1}{2} \sum_{i=1}^N (e_i^k(t))^T e_i^k(t) \end{aligned} \quad (16)$$

Assuming that the suitable $D(q)$ is a positive definite matrix, and according to Assumptions 1 and 2, Equation (16) can be written as:

$$\begin{aligned} \mathcal{L}V^k(t, e^k(t), p) &\leq \sum_{i=1}^N (e_i^k(t))^T \nu P e_i^k(t) - \sum_{i=1}^N (e_i^k(t))^T \eta_i(p) e_i^k(t) \\ &\quad + \frac{1}{2} \rho_i^k(p) \sum_{i=1}^N (e_i^k(t))^T e_i^k(t) - \varphi(p) \sum_{i=1}^N (e_i^k(t))^T \text{sign}(e_i^k(t)) |e_i^k(t)|^\beta \\ &\quad + \sum_{q=1}^m \pi_{pq} \frac{1}{2} \sum_{i=1}^N (e_i^k(t))^T D(q) e_i^k(t) + c_1 \sum_{i=1}^N (e_i^k(t))^T \sum_{j=1}^N a_{ij}(p) \Gamma_1 e_j^k(t) \\ &\quad + c_2 \sum_{i=1}^N (e_i^k(t))^T \sum_{j=1}^N b_{ij}(p) \Gamma_2 e_j^k(t) \end{aligned} \quad (17)$$

Based on Lemma 1, we can get

$$\begin{aligned} - \sum_{i=1}^N (e_i^k(t))^T \text{sign}(e_i^k(t)) |e_i^k(t)|^\beta &= - \sum_{i=1}^N (e_i^k(t))^T \text{diag}\{\text{sign}(e_{i1}^k(t)), \dots, \text{sign}(e_{in}^k(t))\} |e_i^k(t)|^\beta \\ &= - \sum_{i=1}^N \sum_{j=1}^N e_{ij}^k(t) |e_{ij}^k(t)|^\beta \text{sign}(e_{ij}^k(t)) = - \sum_{i=1}^N \sum_{j=1}^N |e_{ij}^k(t)|^{1+\beta} \\ &\leq - \left(\sum_{i=1}^N \sum_{j=1}^N |e_{ij}^k(t)|^2 \right)^{\frac{1+\beta}{2}} = - \left(\sum_{i=1}^N e_i^T(t) e_i^k(t) \right)^{\frac{1+\beta}{2}} \end{aligned} \quad (18)$$

Then, inequality (17) can be further reduced to

$$\begin{aligned} \mathcal{L}V^k(t, e^k(t), p) &\leq \sum_{i=1}^N (e_i^k(t))^T \left[\Omega + \Lambda + \hat{A} + \hat{B} - \left(\frac{1}{2} \Theta(p) - \Xi(p) \right) \otimes I_N \right] e_i^k(t) \\ &\quad + \sum_{q=1}^m \pi_{pq} \frac{1}{2} \sum_{i=1}^N (e_i^k(t))^T (D(q) - Q(p)) e_i^k(t) - \varphi(p) \left(\sum_{i=1}^N (e_i^k(t))^T e_i^k(t) \right)^{\frac{1+\beta}{2}} \end{aligned} \quad (19)$$

For any suitable dimension matrix $Q(p) = Q^T(p) (p \in S)$, have $\sum_{q=1}^m \pi_{pq} Q(p) = 0$. Then denote $v_p = \sum_{q=1}^m \frac{\pi_{pq}(D(q) - Q(p))}{2}$. Therefore, from Lemma 1 we have

$$\mathcal{L}V^k(t, e^k(t), p) \leq -\varphi(p) \left(\sum_{i=1}^N e_i^T(t) e_i^k(t) \right)^{\frac{1+\beta}{2}} = -\varphi(p) 2^{\frac{1+\beta}{2}} \mathcal{L}V^k(t, e^k(t), p)^{\frac{1+\beta}{2}} \quad (20)$$

According to (12), denote $\gamma = (1 + \beta)/2$, then taking the expectation on both sides of Equation (20), we have

$$\mathcal{E} \left[\mathcal{L}V^k(t, e^k(t), p) \right] \leq -\varphi 2^\gamma \mathcal{E} \left[V^k(t, e^k(t), p) \right]^\gamma \quad (21)$$

Assume that there exists a positive constant ϱ that satisfies $\mathcal{E} \left[V^k(t_0, e^k(t_0), p) \right]^\gamma \geq \varrho \left(\mathcal{E} \left[V^k(t_0, e^k(t_0), p) \right] \right)^\gamma$ and denote $\mu = \varphi \varrho$. Thus

$$\mathcal{E} \left[\mathcal{L}V^k(t, e^k(t), p) \right] \leq -\mu 2^\gamma \left(\mathcal{E} \left[V^k(t, e^k(t), p) \right] \right)^\gamma \quad (22)$$

We integrate both sides of inequality (22) in the time interval $(t_{k-1}, t_k]$, and we then have

$$\mathcal{E} \left(\left[V^k(t_k, e^k(t_k), r(t_k)) \right]^{1-\gamma} \right) \leq \mathcal{E} \left(\left[V^{k-1}(t_{k-1}, e^{k-1}(t_{k-1}), r(t_{k-1})) \right]^{1-\gamma} \right) - \mu 2^\gamma (1 - \gamma) (t_k - t_{k-1}) \quad (23)$$

Then, in the time interval $(t_{k-1}, t_k]$, we have

$$t_k - t_{k-1} \leq \frac{\mathcal{E}([V^{k-1}(t_{k-1}, e^{k-1}(t_{k-1}), r(t_{k-1}))])^{1-\gamma} - \mathcal{E}([V^k(t_k, e^k(t_k), r(t_k))])^{1-\gamma}}{\mu 2^\gamma (1-\gamma)} \tag{24}$$

In the time interval $(t_{k-2}, t_{k-1}]$ we have

$$t_{k-1} - t_{k-2} \leq \frac{\mathcal{E}([V^{k-2}(t_{k-2}, e^{k-2}(t_{k-2}), r(t_{k-2}))])^{1-\gamma} - \mathcal{E}([V^{k-1}(t_{k-1}, e^{k-1}(t_{k-1}), r(t_{k-1}))])^{1-\gamma}}{\mu 2^\gamma (1-\gamma)} \tag{25}$$

Similarly, the inequalities in $(t_{k-3}, t_{k-2}]$, $(t_{k-4}, t_{k-3}]$, \dots , $(t_1, t_2]$, $(t_0, t_1]$ can be obtained. We add $k + 1$ inequalities to get

$$t_\delta - t_0 \leq \frac{\mathcal{E}([V^0(t_0, e^0(t_0), r(t_0))])^{1-\gamma} - \mathcal{E}([V^\delta(t_k, e^k(t_k), r(t_k))])^{1-\gamma}}{\mu 2^\gamma (1-\gamma)} \tag{26}$$

Then, when $\Delta \rightarrow \infty$, we have

$$t - t_0 \leq \frac{\mathcal{E}([V(t_0, e(t_0), r(t_0))])^{1-\gamma} - \mathcal{E}([V(t, e(t), r(t))])^{1-\gamma}}{\mu 2^\gamma (1-\gamma)} \tag{27}$$

If $V(t, e(t), r(t)) = 0$ exists for any t_0 , the $V(t)$ will converge to zero in a finite time t^* . Therefore, the finite time t^* at $t_0 = 0$ can be estimated by

$$t^* \leq \frac{V(0, r(0))^{1-\gamma}}{\mu 2^\gamma (1-\gamma)} \tag{28}$$

where $V(0, r(0)) = \frac{1}{2} \sum_{i=1}^N e_i^T(0)e_i(0)$. Hence, the synchronization of multi-weight Markovian switching complex network (3) under the optimal node selection strategy can be achieved in a finite time t^* .

The proof is completed. \square

Remark 1. The speed of network synchronization depends on the parameters $\eta(r(t))$ and $\varphi(r(t))$ in the controller (11). Moreover, the inequality (12) in Theorem 1 is a sufficient condition rather than a necessary condition to achieve finite-time synchronization of Markovian switching complex network via the optimal node selection strategy.

4. Finite-Time Synchronization of Markovian Switching Complex Networks Based on Event-Triggered Control Strategy

In the previous section, the node selection method based on the traction control strategy is proposed and the sufficient conditions for the network to achieve finite time synchronization are obtained. This section will mainly design an effective trigger function and construct an event-triggered control strategy based on this with low control cost and low energy loss to achieve the synchronization of the network.

The first l nodes of the network are selected as controlled nodes in this section, then the error equation of the network can be written as:

$$\begin{cases} \dot{e}_i(t) = f(x_i(t)) - f(s(t)) + c_1 \sum_{j=1}^N a_{ij}(r(t))\Gamma_1 e_j(t) + c_2 \sum_{j=1}^N b_{ij}(r(t))\Gamma_2 e_j(t) \\ \quad + \sigma_i(t, e_i(t), r(t))\dot{\omega}(t) + u_i, \quad i = 1, 2, \dots, l \\ \dot{e}_i(t) = f(x_i(t)) - f(s(t)) + c_1 \sum_{j=1}^N a_{ij}(r(t))\Gamma_1 e_j(t) + c_2 \sum_{j=1}^N b_{ij}(r(t))\Gamma_2 e_j(t) \\ \quad + \sigma_i(t, e_i(t), r(t))\dot{\omega}(t), \quad i = l + 1, l + 2, \dots, N \end{cases} \tag{29}$$

Theorem 2. We aim to design proper event-triggered control scheme, which can effectively ensure the networks (3) to realize finite-time synchronization. In the following, the triggered time sequence of the i -th node is assumed to be $t_i^0 = 0, t_i^1, t_i^2, \dots, t_i^k, \dots$. Then, we can design the following event-triggered control protocol:

$$\begin{cases} u_i(t_i^k) = -\eta_i(r(t_i^k))e_i(t_i^k) - \varphi(r(t_i^k)\text{sign}(e_i(t_i^k)))|e_i(t_i^k)|_\beta, & \text{if } e_i(t_i^k) \neq 0 \\ u_i(t_i^k) = 0, & \text{if } e_i(t_i^k) = 0 \\ i = 1, 2, \dots, l; & t_i^k \leq t < t_i^{k+1} \end{cases} \quad (30)$$

where control parameters $\eta_i(r(t_i^k))$ and $\varphi(r(t_i^k))$ are positive constants, $r \in \mathbb{C}$; $e_i(t_i^k)$ is the systematic error of the i -th agent at time t_k ; t_i^k is the latest triggered time instant of node i at time t ; $\text{sign}(e_i(t_i^k)) = \text{diag}\{\text{sign}(e_{i1}(t_{i1}^k)), \text{sign}(e_{i2}(t_{i2}^k)), \dots, \text{sign}(e_{in}(t_{in}^k))\}$. Then the control law of node i can be continuously updated at its own event time t_i^k until the network is synchronized. However, under the action of the pinning control strategy, we only need to control a small number of nodes in the network to achieve network synchronization.

According to the established event-triggered controller, a reasonable and reliable trigger function is designed, so that the network can be continuously updated according to certain conditions in the process of achieving consistency. Then, the event trigger function of the agent in any time interval $[t_k, t_{k+1})$ can be designed as follows:

$$g_i(t) = e_i(t_i^k) - e_i(t); \quad \tilde{g}_i(t) = |g_i(t)| - \zeta |e_i(t)| \quad (31)$$

where $g_i(t)$ is defined by the measurement error of node i , ζ ($0 < \zeta < 1$) is the control parameter of the trigger function, then the trigger moment of agent i can be set according to the above triggering rules:

$$t_i^{k+1} = \inf\{t > t_i^k, \tilde{g}_i(t) > 0\} \quad (32)$$

Obviously, when the set trigger function is satisfied, the i -th node in the network will retrigger the event and update the controller in the network synchronization process, i.e., $\tilde{g}_i(t) > 0$. This also means that $\tilde{g}_i(t) \leq 0$ always holds in the time interval $[t_k, t_{k+1})$. In addition, when the value of the control parameter ζ of the trigger function is larger, the set trigger conditions will be more difficult to satisfy and the frequency of controller updates will be reduced, which may affect or even destroy the synchronization behavior of the network; on the contrary, when the value of the control parameter ζ of the trigger function is smaller, the set trigger conditions will be easier to satisfy and the frequency of controller updates will increase, which will increase the control cost of the network. Therefore, in the event triggering control, the selection of the control parameters of the trigger function is particularly important.

According to the designed event-triggered controller, and if the following inequalities are formed

$$\begin{cases} \Omega + \Lambda + \hat{A} + \hat{B} + \left(\frac{1}{2}\hat{\Theta}(r(t)) - \hat{\Xi}(r(t))\right) \otimes I_N \leq 0 \\ \sum_{q=1}^m \pi_{pq}(D(q) - Q(p)) \leq 0 \end{cases} \quad (33)$$

where $\hat{\Theta}(r(t)) = \text{diag}\{\underbrace{\rho_1(r(t)), \dots, \rho_l(r(t))}_{l}, \underbrace{0, \dots, 0}_{N-l}\}$; $\hat{\Xi}(r(t)) = \text{diag}\{\underbrace{\eta_1(r(t)), \dots, \eta_l(r(t))}_{l}, \underbrace{0, \dots, 0}_{N-l}\}$; $I_N = \text{diag}\{\underbrace{1, \dots, 1}_{l}, \underbrace{0, \dots, 0}_{N-l}\}$. The rest of the parameters are the same as defined in Theorem 1. Thus, the synchronization of (3) can be achieved within a finite time t^* .

$$t^* \leq \frac{V(0, r(0))^{1-\gamma}}{\mu 2^\gamma (1-\gamma)} \quad (34)$$

where $\sigma = \min(\varphi(r(t_i^k))(1 - \xi^\beta)2^\gamma)$; $\gamma = (1 + \beta)/2$; $\mu = \varrho \min(\sigma, \lambda/2^{(1+\beta)/2}, 1)$, ϱ is an appropriate positive constant; $V(0, e(0), r(0)) = \frac{1}{2} \sum_{i=1}^N e_i^T(0)e_i(0)$; $e_i(0)$ is the initial condition.

Proof. The Lyapunov function constructed as follows:

$$V(t, e(t), p) = \frac{1}{2} \sum_{i=1}^N e_i^T(t)e_i(t)$$

According to the differential operator L [23], the above Lyapunov function can be written as

$$\begin{aligned} \mathcal{L}V(t, e(t), p) &= \sum_{i=1}^N e_i^T(t)\dot{e}_i(t) + \sum_{q=1}^m \pi_{pq} \frac{1}{2} \sum_{i=1}^N e_i^T(t)e_i(t) \\ &+ \frac{1}{2} \sum_{i=1}^N \left[\text{trace}(\sigma_i^T(t, e_i(t), p)) \sigma_i(t, e_i(t), p) \right] \end{aligned} \quad (35)$$

Bringing the error system (29) and the event-triggered controller (30) into the above equation, we have

$$\begin{aligned} \mathcal{L}V(t, e(t), p) &= \sum_{i=1}^N (e_i(t))^T \left\{ f(t, x_i(t)) - f(t, s(t)) - \varphi(p) \text{sign}(e_i(t_i^k)) |e_i(t_i^k)|^k \right. \\ &\quad \left. - \eta_i(p)e_i(t_i^k) + c_1 \sum_{j=1}^N a_{ij}(p)\Gamma_1 e_j(t) + c_2 \sum_{j=1}^N b_{ij}(p)\Gamma_2 e_j(t) \right\} \\ &+ \frac{1}{2} \sum_{i=1}^N \left[\text{trace}(\sigma_i^T(t, e_i(t), p)) \sigma_i(t, e_i(t), p) \right] + \frac{1}{2} \sum_{q=1}^m \pi_{pq} \sum_{i=1}^N e_i^T(t)e_i(t) \end{aligned} \quad (36)$$

Based on the above theoretical analysis to the process, the above inequality can be further simplified as:

$$\begin{aligned} \mathcal{L}V(t, e(t), p) &\leq \sum_{i=1}^N e_i^T(t) \nu P e_i(t) - \sum_{i=1}^N e_i^T(t) \eta_i(p) e_i(t_i^k) + \frac{1}{2} \rho_i(p) \sum_{i=1}^N e_i^T(t) e_i(t) \\ &\quad - \varphi(p) \sum_{i=1}^N e_i^T(t) \text{sign}(e_i(t_i^k)) |e_i(t_i^k)|^\beta + \frac{1}{2} \sum_{q=1}^m \pi_{pq} \sum_{i=1}^N e_i^T(t) D(q) e_i(t) \\ &\quad + c_1 \sum_{j=1}^N a_{ij}(p) \Gamma_1 e_j(t) + c_2 \sum_{j=1}^N b_{ij}(p) \Gamma_2 e_j(t) \end{aligned} \quad (37)$$

As mentioned above, the event-triggered function (31) implies that the inequality $|g_i(t)| = |e_i(t_i^k) - e_i(t)| \leq \xi |e_i(t)| \leq |e_i(t)| (0 < \xi < 1)$ holds for any time interval $[t_k, t_{k+1})$, thus

$$\begin{aligned} - \sum_{i=1}^N e_i^T(t) e_i(t_i^k) &= - \sum_{i=1}^N e_i^T(t) e_i(t) + \sum_{i=1}^N e_i^T(t) (e_i(t) - e_i(t_i^k)) \\ &\leq -(1 - \xi) \sum_{i=1}^N e_i^T(t) e_i(t) \end{aligned} \quad (38)$$

Meanwhile, the event-triggered function (31) implies $|g_i(t)| \leq |e_i(t)|$, and $e_i(t_k^i) = g_i(t) + e_i(t)$, then $|g_i(t)| \leq |e_i(t)|$ implies that the equation $\text{sign}(e_i(t_k^i)) = \text{sign}(e_i(t))$ holds. According to Lemma 1

$$\begin{aligned} -\sum_{i=1}^N e_i^T(t) \text{sign}(e_i(t_k^i)) |e_i(t_k^i)|^\beta &= -\sum_{i=1}^N |e_i^T(t)| \cdot |e_i(t_k^i)|^\beta \\ &= \sum_{i=1}^N |e_i^T(t)| \cdot (|e_i^T(t)|^\beta - |e_i(t_k^i)|^\beta) - \sum_{i=1}^N |e_i^T(t)| \cdot |e_i^T(t)|^\beta \\ &\leq -\sum_{i=1}^N |e_i^T(t)| \cdot |e_i^T(t)|^\beta + \sum_{i=1}^N |e_i^T(t)| \cdot |e_i^T(t) - e_i(t_k^i)|^\beta \\ &\leq -\sum_{i=1}^N |e_i^T(t)|^{1+\beta} + \zeta^\beta \sum_{i=1}^N |e_i^T(t)|^{1+\beta} = -(1 - \zeta^\beta) \sum_{i=1}^N |e_i^T(t)|^{1+\beta} \end{aligned} \quad (39)$$

Then, the inequality (37) can be further written as

$$\begin{aligned} \mathcal{L}V(t, e(t), p) &\leq \sum_{i=1}^N e_i^T(t) \left[\Omega + \Lambda + \hat{A} + \hat{B} - \left(\frac{1}{2} \hat{\Theta}(p) - \hat{\Xi}(p) \right) \otimes I_N \right] e_i(t) \\ &\quad + \sum_{q=1}^m \pi_{pq} \frac{1}{2} \sum_{i=1}^N e_i^T(t) (D(q) - Q(p)) e_i(t) \\ &\quad - \varphi(p) (1 - \zeta^\beta) \left(\sum_{i=1}^N e_i^T(t) e_i(t) \right)^{\frac{1+\beta}{2}} \end{aligned} \quad (40)$$

For any suitable matrix $Q(p) = Q^T(p) (p \in \mathcal{S})$, have $\sum_{q=1}^m \pi_{pq} Q(p) = 0$, and denote that $v_p = \sum_{q=1}^m \frac{\pi_{pq} (D(q) - Q(p))}{2}$. Therefore, from Lemma 1 we have

$$\mathcal{L}V(t, e(t), p) \leq -\varphi(p) (1 - \zeta^\beta) \left(\sum_{i=1}^N e_i^T(t) e_i(t) \right)^{\frac{1+\beta}{2}} = -\mu' \mathcal{L}V(t, e(t), p)^\gamma \quad (41)$$

where $\mu' = \varphi(p) (1 - \zeta^\beta) 2^\gamma$, $\gamma = (1 + \beta)/2$, according to the sufficient conditions (33) of Theorem 2, then taking the expectation on both sides of Equation (41), we have

$$\mathcal{E}[\mathcal{L}V(t, e(t), p)] \leq -\mu' 2^\gamma \mathcal{E}[V^\gamma(t, e(t), p)] \quad (42)$$

Assume that $\mathcal{E}[V^\gamma(t_0, e(t_0), p)] \geq \varrho (\mathcal{E}[V(t_0, e(t_0), p)])^\gamma$ hold, ϱ is a positive constant that satisfies and denote $\mu = \mu' \varrho$. Thus

$$\mathcal{E}[\mathcal{L}V(t, e(t), p)] \leq -\mu 2^\gamma (\mathcal{E}[V(t, e(t), p)])^\gamma \quad (43)$$

Integrate both sides of inequality (43), we have

$$\mathcal{E}([V(t, e(t), r(t))]^{1-\gamma}) \leq \mathcal{E}([V(t_0, e(t_0), r(t_0))]^{1-\gamma}) - \mu 2^\gamma (1 - \gamma) (t - t_0) \quad (44)$$

Then we can get

$$t - t_0 \leq \frac{\mathcal{E}([V(t_0, e(t_0), r(t_0))]^{1-\gamma}) - \mathcal{E}([V(t, e(t), r(t))]^{1-\gamma})}{\mu 2^\gamma (1 - \gamma)} \quad (45)$$

If $V(t, e(t), r(t)) = 0$ exists for any t_0 , the $V(t)$ will converge to zero in a finite time t^* . Therefore, the finite time t^* at $t_0 = 0$ can be estimated by

$$t^* \leq \frac{V(0, r(0))^{1-\gamma}}{\mu 2^\gamma (1 - \gamma)} \quad (46)$$

where $V(0, r(0)) = \frac{1}{2} \sum_{i=1}^N e_i^T(0) e_i(0)$.

Hence, the synchronization of Markovian switching complex networks under the event-triggered control strategy can be achieved in a finite time t^* .

The proof is completed. \square

Remark 2. Based on the event-triggered control strategy proposed in Theorem 2, the control cost and energy loss can be reduced while ensuring synchronization. Moreover, the inequality (33) in Theorem 2 is a sufficient condition rather than a necessary condition to achieve finite-time synchronization of Markovian switching complex network via the event-triggered control strategy.

Remark 3. The trigger function designed in this section implies that the trigger function (31) will not be satisfied in any time interval $t \in [t^k, t^{k+1})$, i.e., $\tilde{g}(t) \leq 0$. When the trigger condition is satisfied by the i -th node, the network will automatically trigger the function and update the controller into the next time interval $t \in [t^{k+1}, t^{k+2})$ to continue the trigger control until the network achieves synchronization, and the trigger function (31) will not be satisfied again at that time.

5. Illustrative Examples

This paper proposes the optimal node selection strategy and an event-triggered control strategy for synchronization control of Markovian switching complex networks, both of which are low energy cost control schemes. The control energy cost mainly considers the number of control nodes. The smaller the number of control nodes, the lower the energy cost. In addition, in order to optimally achieve synchronization control under low energy cost mechanism, a control strategy with faster synchronization speed and fewer control nodes is better.

In this section, two sets of comparative simulations will be performed to verify the correctness and effectiveness of the optimal node selection strategy and event-triggered control strategy, and the advantages of the two control strategies proposed in this paper will be analyzed through the simulation results.

Example 1. The node system of complex network is described by the chaotic system (47).

$$\begin{cases} \dot{x}_{i1}(t) = -x_{i1}(t) - x_{i2}(t)x_{i3}(t) + 20x_{i3}(t) \\ \dot{x}_{i2}(t) = -x_{i2}(t) + x_{i1}(t)x_{i3}(t) \\ \dot{x}_{i3}(t) = 5.45(x_{i1}(t) - x_{i3}(t)) \end{cases} \quad i = 1, 2, \dots, N \quad (47)$$

This numerical simulation will compare the proposed optimal node selection strategy and event-triggered control strategy by numerical simulation of 20 nodes. In this simulation, the complex network, switching mode, and all parameters will remain consistent. The switching of two different modes in the complex network are shown in Figure 1, and the parameters of the network are also given in the following:

$$\Gamma_1 = \begin{bmatrix} 0.5 & 0 & 0 \\ 0 & 0.5 & 0 \\ 0 & 0 & 0.5 \end{bmatrix}, \Gamma_2 = \begin{bmatrix} 0.8 & 0 & 0 \\ 0 & 0.8 & 0 \\ 0 & 0 & 0.8 \end{bmatrix}, \Pi = \begin{bmatrix} -2 & 2 \\ 1 & -1 \end{bmatrix},$$

$$\sigma_i(t, e_i(t), 1) = \text{diag} \left\{ \frac{\sqrt{2}}{2} e_{i1}(t), \frac{\sqrt{2}}{2} e_{i2}(t), \frac{\sqrt{2}}{2} e_{i3}(t) \right\}$$

$$\sigma_i(t, e_i(t), 2) = \text{diag} \left\{ \sqrt{2} e_{i1}(t), \sqrt{2} e_{i2}(t), \sqrt{2} e_{i3}(t) \right\}.$$

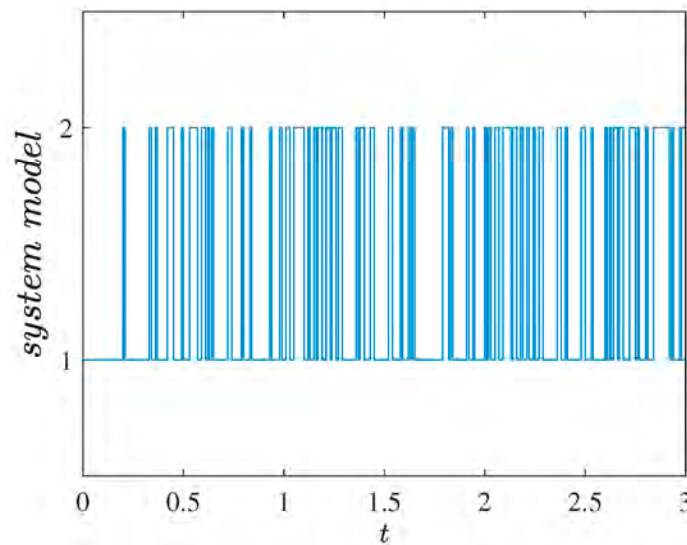


Figure 1. Switching of the network mode.

Example 2. Finite-time synchronization of a multi-weighted Markovian switching complex network will be achieved by the optimal node selection strategy under different coupling strengths ($c_1 = c_2 = 10, 1, 0.1, 0.001$). The maximum average error node in each time interval $(t_{k-1}, t_k]$ is selected as the control node. That is, only one node in the network is selected as the controlled node in this simulation, i.e., $u_i(t) = (u_1(t), \overbrace{0, 0, \dots, 0}^{20-1})$, then the other control parameters in Theorem 1 are: $\eta(1) = 90, \eta(2) = 100; \varphi(1) = 50, \varphi(2) = 45; \beta = 0.6; \Xi(1) = (90, \overbrace{0, 0, \dots, 0}^{20-1}), \Xi(2) = (100, \overbrace{0, 0, \dots, 0}^{20-1}); \rho(1) = 2, \rho(2) = 1.25$. According to (13), we can get $t^* \leq 8.3147$ by simple calculation.

The evolution curves of the network synchronization error with time for different coupling strengths ($c_1 = c_2 = 10, 1, 0.1, 0.001$) are given in Figures 2–5, respectively, from which it can be seen that the network synchronization error $e_i(t)$ basically converges to 0 at $t \approx 0.6$; Figures 6–9 show the update process of the pinning controller with time for different coupling strengths ($c_1 = c_2 = 10, 1, 0.1, 0.001$), from which it can be seen that the designed controller $u_i(t)$ are also gradually updated to zero at $t \approx 0.6$. Then the synchronization of the multi-weight Markovian switching network can be achieved approximately at $t \approx 0.6$. Therefore, under the optimal node selection strategy, when the coupling strength of the complex network changes, the synchronization time of the network does not change significantly.

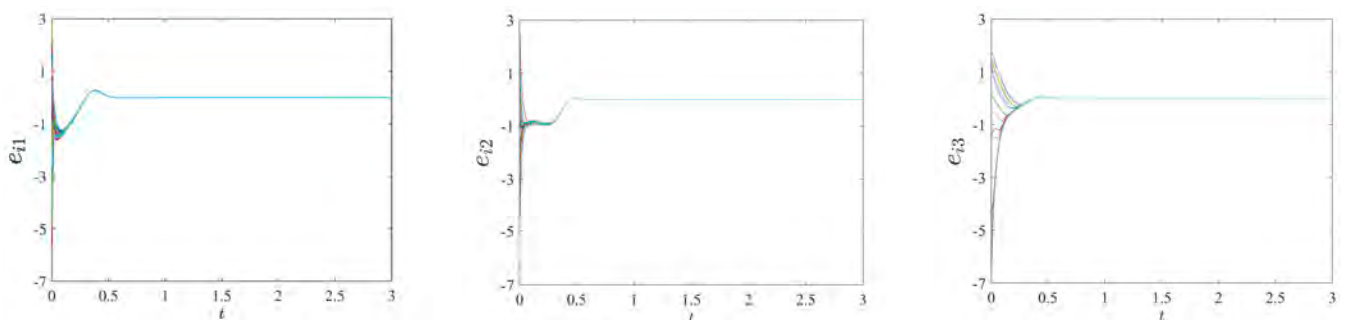


Figure 2. The synchronization error $e_i(t)$ of the network ($c_1 = c_2 = 10$).

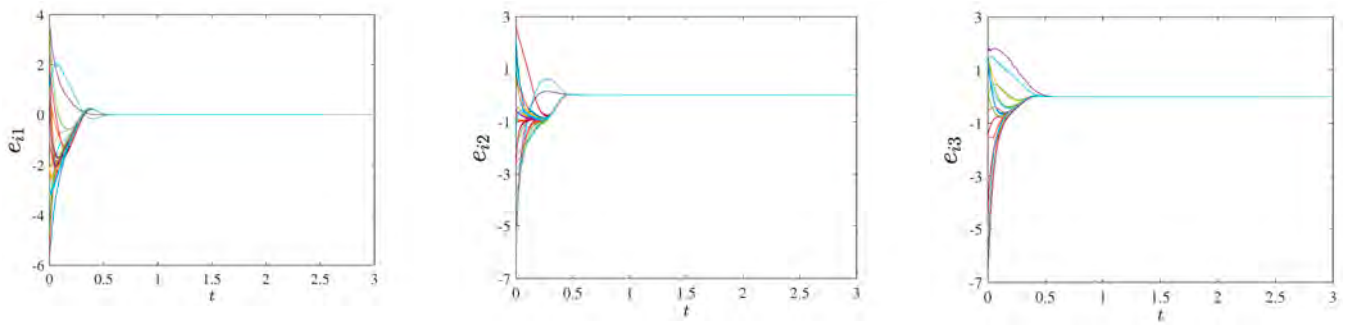


Figure 3. The synchronization error $e_i(t)$ of the network ($c_1 = c_2 = 1$).

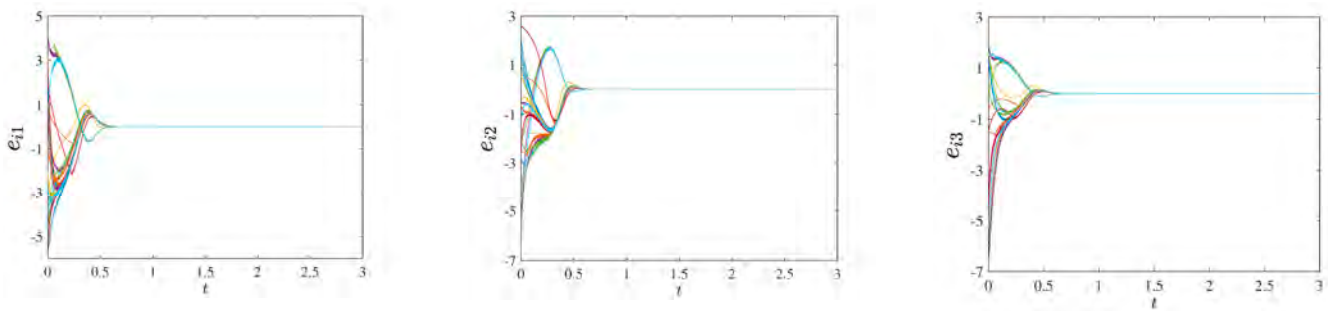


Figure 4. The synchronization error $e_i(t)$ of the network ($c_1 = c_2 = 0.1$).

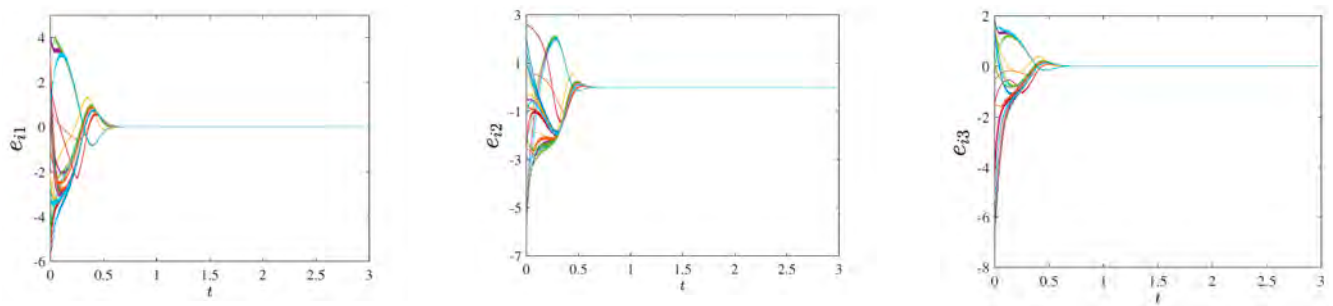


Figure 5. The synchronization error $e_i(t)$ of the network ($c_1 = c_2 = 0.001$).

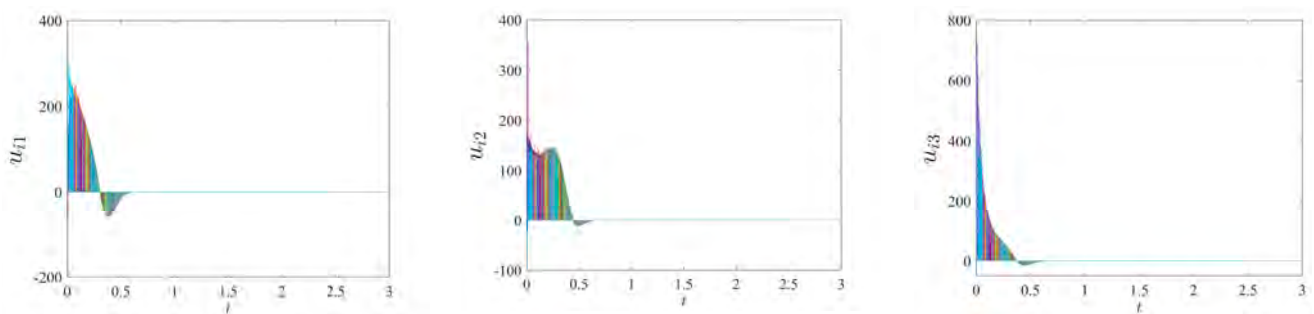


Figure 6. The update process of pinning controller $u_i(t)$ with time ($c_1 = c_2 = 10$).

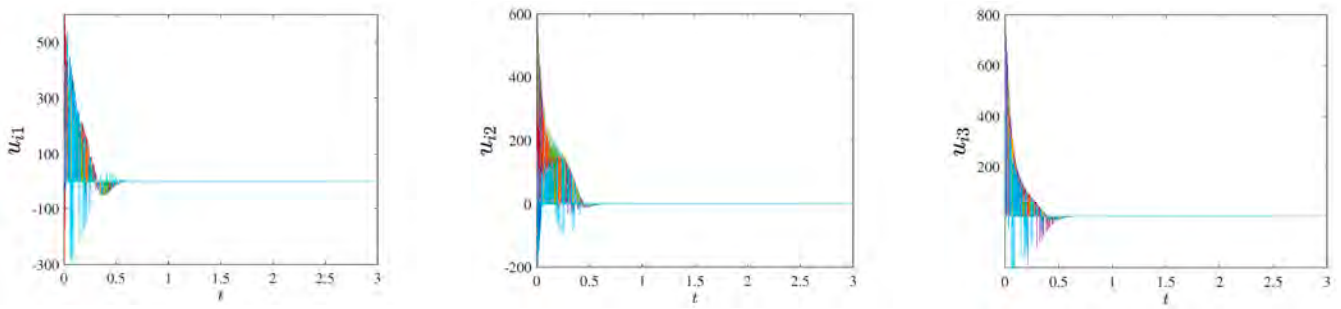


Figure 7. The update process of pinning controller $u_i(t)$ with time ($c_1 = c_2 = 1$).

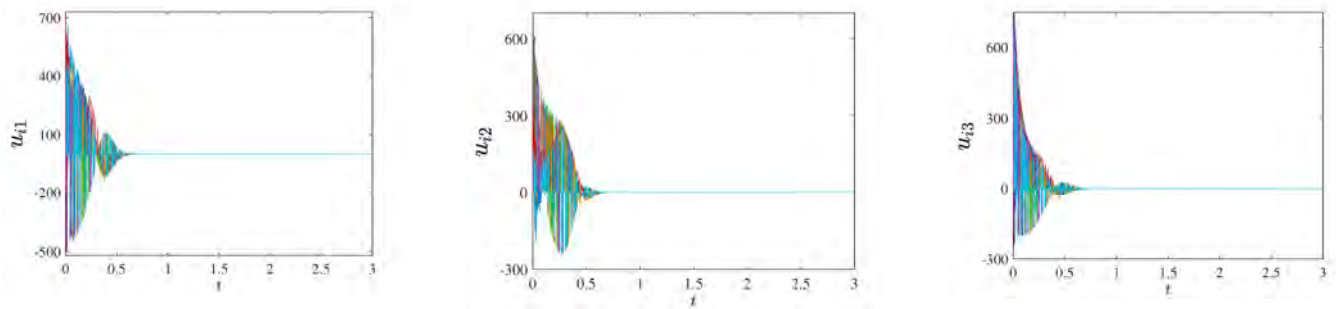


Figure 8. The update process of pinning controller $u_i(t)$ with time ($c_1 = c_2 = 0.1$).

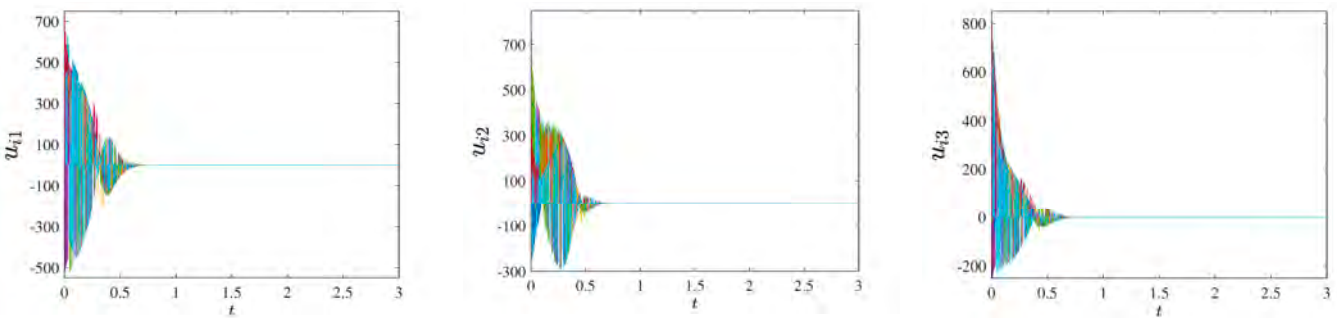


Figure 9. The update process of pinning controller $u_i(t)$ with time ($c_1 = c_2 = 0.001$).

In general, synchronization of complex networks can be achieved with very few of the control nodes when the coupling strength is large enough, or with a sufficient number of control nodes when the coupling strength is small. For the optimal node selection strategy proposed in this paper, not only the synchronization control of the complex network with Markovian switching is achieved with weak coupling strength ($c_1 = c_2 = 0.001$) and very few controlled nodes (1 controlled node), but also the synchronization efficiency of the network is improved, thus reducing the energy cost of the network.

Example 3. In this simulation, finite-time synchronization of Markovian switching complex network will be achieved by the event-triggered control strategy under different coupling strengths ($c_1 = c_2 = 10, 1, 0.4$). According to the established event-triggered function to update the controller at all synchronization times, and the three nodes of the network are selected as controlled nodes,

i.e., $u_i(t) = (\overbrace{(u_1(t), u_2(t), u_3(t))}^3, \overbrace{0, 0, \dots, 0}^{20-3})$. The parameter values in Theorem 2 are the same as those in Theorem 1. Especially, the control parameter ξ of the trigger function (31) is taken as

$\xi = 0.7$; $\Xi(1) = (\overbrace{90, 72, 88}^3, \overbrace{0, 0, \dots, 0}^{20-3})$, $\Xi(2) = (\overbrace{101, 83, 98}^3, \overbrace{0, 0, \dots, 0}^{20-3})$. According to (34), we can get $t^* \leq 9.4628$ by simple calculation.

The evolution curves of the network synchronization error with time for different coupling strengths ($c_1 = c_2 = 10, 0.1, 0.4$) are given by Figures 10–12 respectively; the update process of the event-triggered controller with time for different coupling strengths ($c_1 = c_2 = 10, 0.1, 0.4$) is given by Figures 13–15, respectively. We can find that the synchronization error curves and the controller update curves of the system converge to zero at different network coupling strengths ($c_1 = c_2 = 10, 1, 0.4$) are different. Where synchronization of the Markovian switching network can be achieved at $t \approx 0.2$ when the coupling strength $c_1 = c_2 = 10$, at $t \approx 1.2$ when the coupling strength $c_1 = c_2 = 1$, at $t \approx 5$ when the coupling strength $c_1 = c_2 = 0.4$. When the coupling strength of the network is very weak (less than 0.1 in Example 3), the Markovian complex network will no longer be synchronized under the event-triggered control strategy. Therefore, under the event-triggered control strategy, the synchronization time of the network gradually increases as the coupling strength of the network decreases.

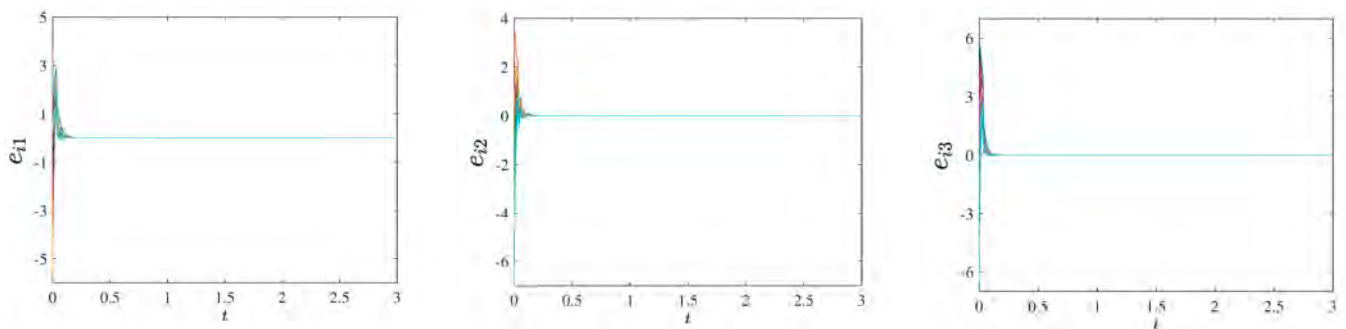


Figure 10. The synchronization error $e_i(t)$ of the network ($c_1 = c_2 = 10$).

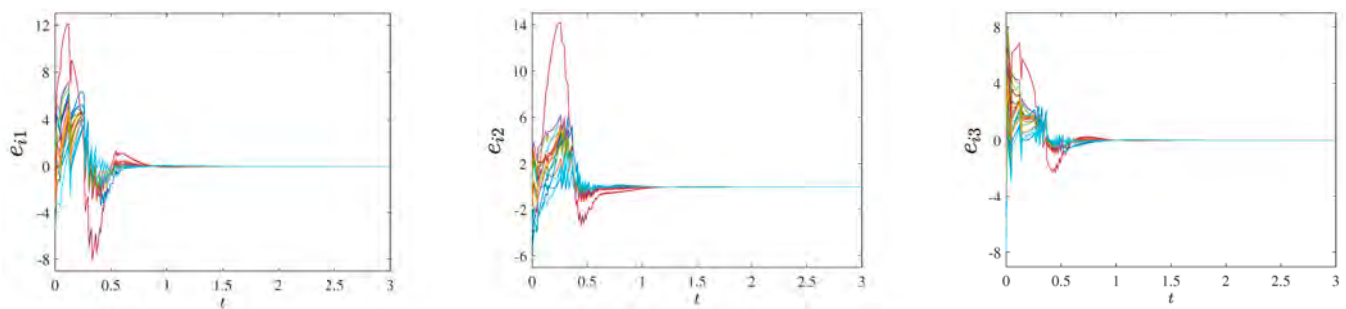


Figure 11. The synchronization error $e_i(t)$ of the network ($c_1 = c_2 = 1$).

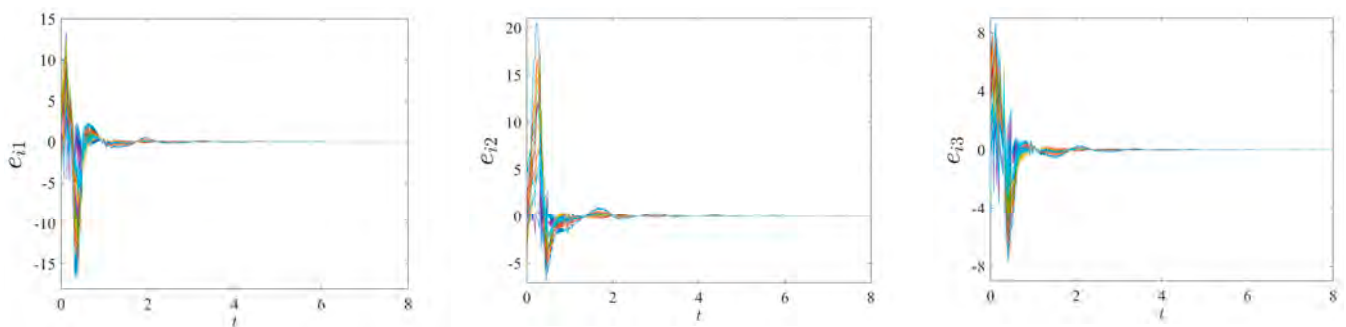


Figure 12. The synchronization error $e_i(t)$ of the network ($c_1 = c_2 = 0.4$).

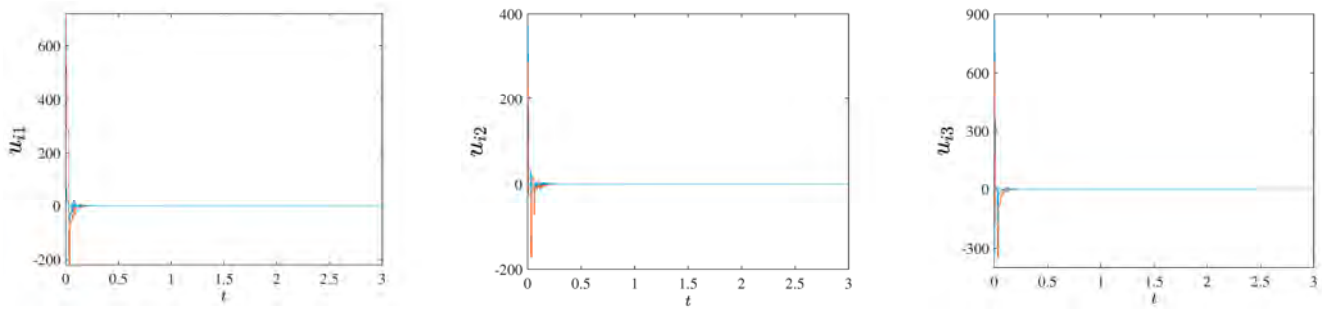


Figure 13. The update process of event-triggered controller $u_i(t)$ with time ($c_1 = c_2 = 10$).

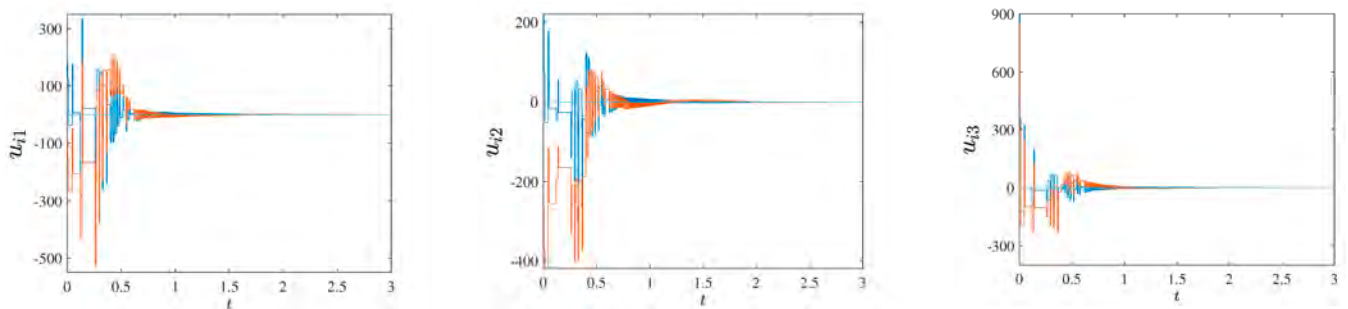


Figure 14. The update process of event-triggered controller $u_i(t)$ with time ($c_1 = c_2 = 1$).

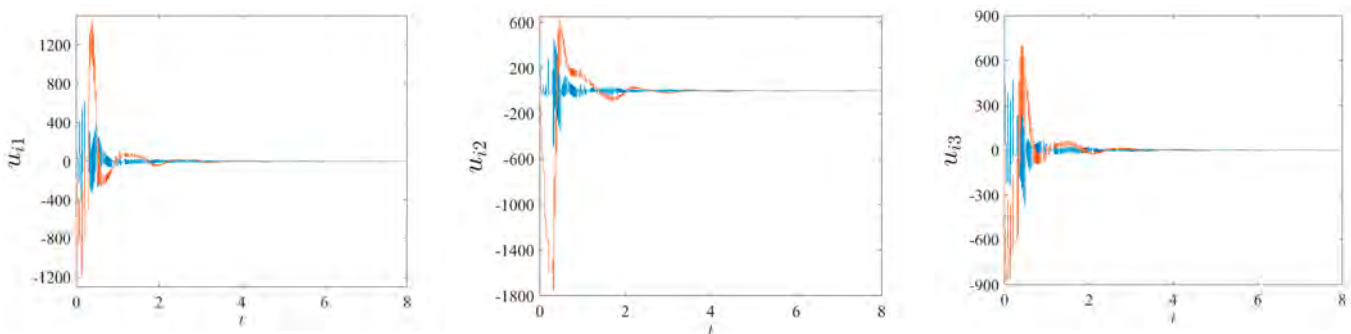


Figure 15. The update process of event-triggered controller $u_i(t)$ with time ($c_1 = c_2 = 0.4$).

The update process of the event-triggered controller is stepped, which is completely consistent with Remark 3. When the controller remains consistent, it means that the event trigger function condition is not satisfied, and the controller of the network remains unchanged at this time. When the controller appears to step up or down, it means that the set event trigger function is satisfied, and the controller of the network is updated at this time; thus, the theoretical analysis and the simulation results are also mutually verified.

Table 1 shows the comparison of the synchronization time of the two control strategies in Example 1 (20-nodes network) with different coupling strengths.

Table 1. Comparison of the synchronization time of two control strategies in Example 1.

Control Strategy	Coupling Strength	Synchronization Time
Optimal node selection	$(c_1 = c_2 = 10)$	$t \approx 0.6$
Event trigger control	$(c_1 = c_2 = 10)$	$t \approx 0.2$
Optimal node selection	$(c_1 = c_2 = 1)$	$t \approx 0.6$
Event trigger control	$(c_1 = c_2 = 1)$	$t \approx 1.2$
Optimal node selection	$(c_1 = c_2 = 0.1)$	$t \approx 0.6$
Event trigger control	$(c_1 = c_2 = 0.1)$	/
Event trigger control	$(c_1 = c_2 = 0.4)$	$t \approx 5$
Optimal node selection	$(c_1 = c_2 = 0.01)$	$t \approx 0.6$
Event trigger control	$(c_1 = c_2 = 0.01)$	/

The following conclusions can be obtained by analyzing the simulation results of Examples 2 and 3. When the network coupling is large enough ($c_1 = c_2 = 10$), the event-triggered control can achieve the synchronization of the network faster. When the coupling strength of the network gradually decreases ($c_1 = c_2 = 1$), the optimal node selection strategy can achieve the synchronization of the network faster. When the coupling strength of the network continues to decrease again ($c_1 = c_2 = 0.1$), the multi-weight Markovian switching complex network will no longer be able to achieve synchronization under the event-triggered control strategy. Moreover, the event-triggered control strategy controls three nodes of the network to achieve network synchronization, while the optimal node selection strategy only needs to control one node to achieve network synchronization, which can also reduce the control cost of the network. Therefore, when the actual system needs to achieve fast network synchronization with low control cost, the optimal node selection strategy can be used. When the actual system is not concerned with control cost but only needs to achieve faster network synchronization, the event-triggered control method can be used.

Example 4. The node system of complex network is described by the Lorenz system (48).

$$\begin{cases} \dot{x}_{i1}(t) = 10(x_{i2}(t) - x_{i1}(t)) \\ \dot{x}_{i2}(t) = 28x_{i1}(t) - x_{i1}(t)x_{i3}(t) - x_{i2}(t) \\ \dot{x}_{i3}(t) = x_{i1}(t)x_{i2}(t) - \frac{8}{3}x_{i3}(t) \end{cases} \quad i = 1, 2, \dots, N \quad (48)$$

In order to further illustrate the advantages of the optimal node selection strategy and the event-triggered control strategy, this section will adopt the 100-node Markovian switching complex network model for simulation. In this simulation, the complex network, switching mode and all parameters will remain consistent. The switching of two different modes in the complex network can be shown in Figure 16, and the parameters of the network are also given below.

$$\Gamma_1 = \begin{bmatrix} 0.8 & 0 & 0 \\ 0 & 0.8 & 0 \\ 0 & 0 & 0.8 \end{bmatrix}, \Gamma_2 = \begin{bmatrix} 1 & 0 & 0 \\ 0 & 1 & 0 \\ 0 & 0 & 1 \end{bmatrix}, \Pi = \begin{bmatrix} -2 & 2 \\ 1 & -1 \end{bmatrix},$$

$$\sigma_i(t, e_i(t), 1) = \text{diag} \left\{ \frac{\sqrt{2}}{2} e_{i1}(t), \frac{\sqrt{2}}{2} e_{i2}(t), \frac{\sqrt{2}}{2} e_{i3}(t) \right\}$$

$$\sigma_i(t, e_i(t), 2) = \text{diag} \left\{ \sqrt{2} e_{i1}(t), \sqrt{2} e_{i2}(t), \sqrt{2} e_{i3}(t) \right\}$$

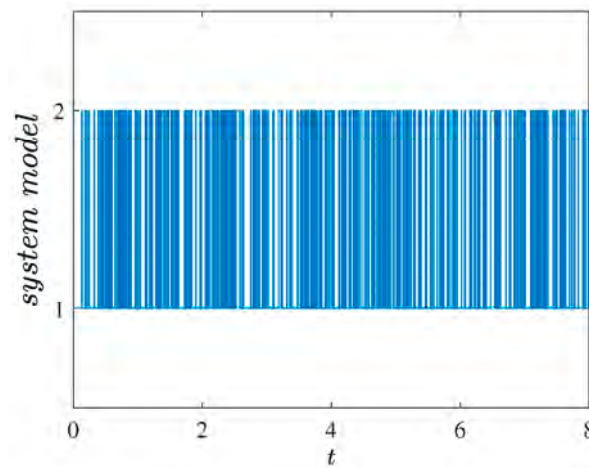


Figure 16. Switching of network mode.

Example 5. In this example, a multi-weight Markovian switching complex network model simulation with 100 nodes was performed using the optimal node selection strategy, and the coupling strengths of the networks were $c_1 = c_2 = 10$, $c_1 = c_2 = 1$, $c_1 = c_2 = 0.1$ and $c_1 = c_2 = 0.001$, respectively. The maximum average error node (only one node) in each time interval $(t_{k-1}, t_k]$ is selected as the controlled node in this simulation, i.e., $u_i(t) = (u_1(t), \overbrace{0, 0, \dots, 0}^{100-1})$, then the other control parameters in Theorem 1 are: $\eta(1) = 90$, $\eta(2) = 100$; $\varphi(1) = 50$, $\varphi(2) = 45$; $\beta = 0.6$; $\Xi(1) = (\overbrace{90, 0, 0, \dots, 0}^{100-1})$, $\Xi(2) = (\overbrace{100, 0, 0, \dots, 0}^{100-1})$; $\rho(1) = 2$, $\rho(2) = 1.25$. According to (13), we can get $t^* \leq 9.1316$ by simple calculation.

Figures 17–24 show the network synchronization error curves and the pinning controller evolution process under different coupling strengths ($c_1 = c_2 = 10, 1, 0.1, 0.001$), respectively, from which it can be seen that the multi-weight Markovian switching complex network basically converges to zero at $t \approx 4$. This again verifies the conclusion obtained in Example 2. Based on the optimal node selection strategy, on the one hand, the network synchronization time does not change significantly with the change of the network coupling strength. On the other hand, synchronization can be achieved under weak coupling strength ($c_1 = c_2 = 0.001$) and very few controlled nodes (1 controlled node), which further reduces the network energy loss and control cost.

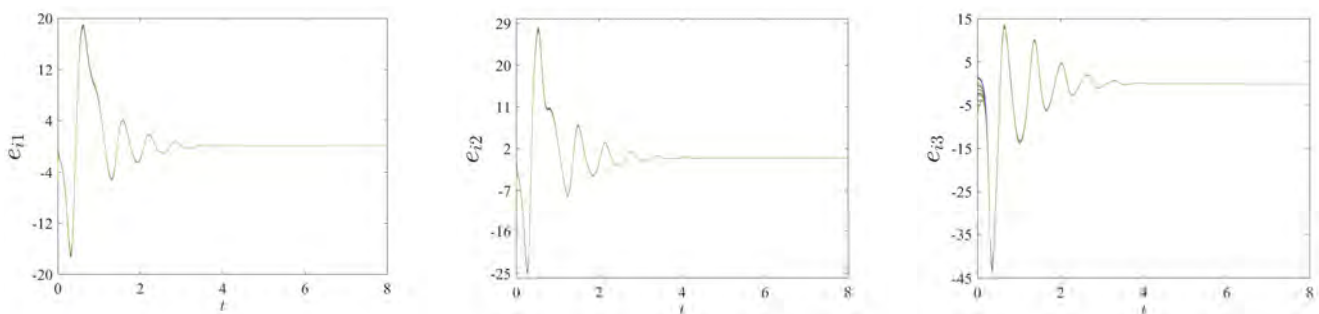


Figure 17. The synchronization error $e_i(t)$ of the network ($c_1 = c_2 = 10$).

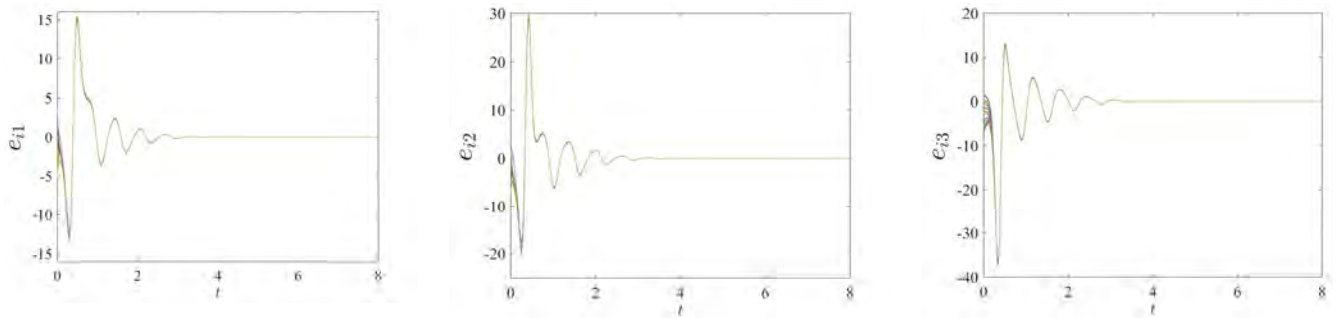


Figure 18. The synchronization error $e_i(t)$ of the network ($c_1 = c_2 = 1$).

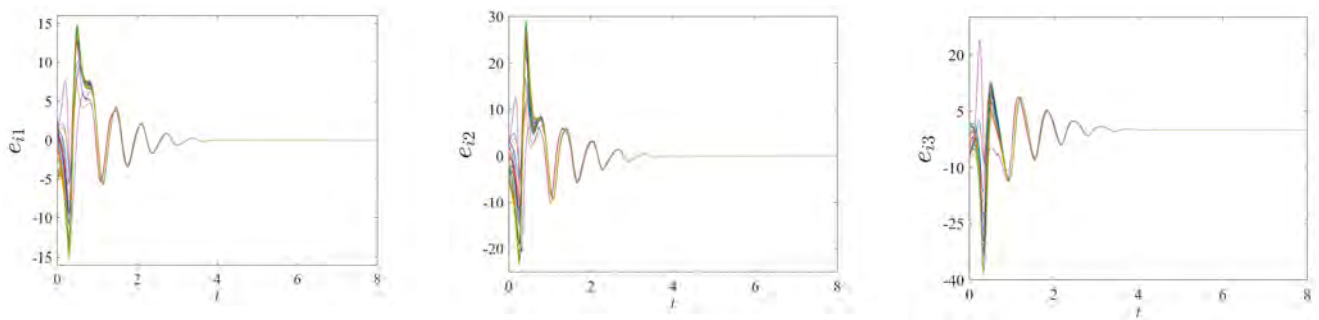


Figure 19. The synchronization error $e_i(t)$ of the network ($c_1 = c_2 = 0.1$).

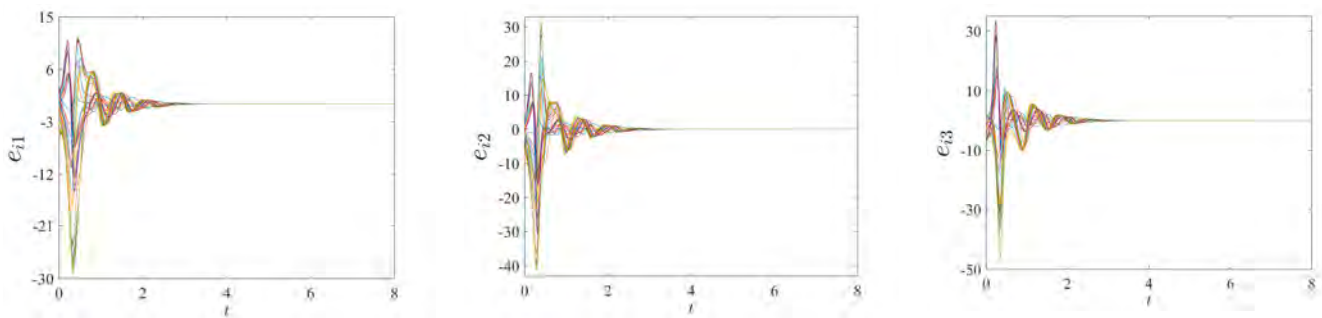


Figure 20. The synchronization error $e_i(t)$ of the network ($c_1 = c_2 = 0.001$).

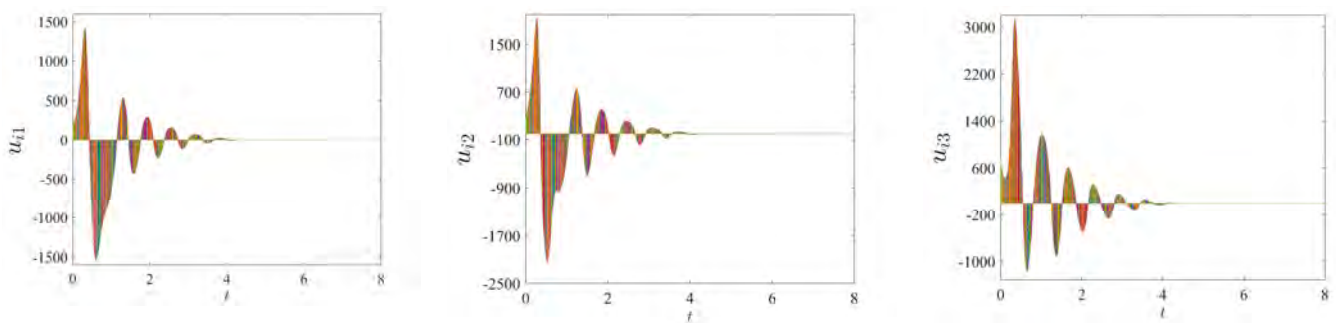


Figure 21. The update process of pinning controller $u_i(t)$ with time ($c_1 = c_2 = 10$).

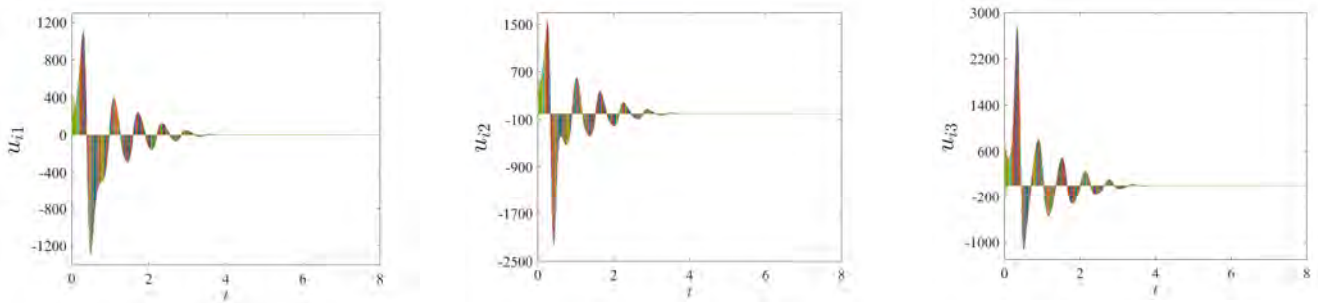


Figure 22. The update process of pinning controller $u_i(t)$ with time ($c_1 = c_2 = 1$).

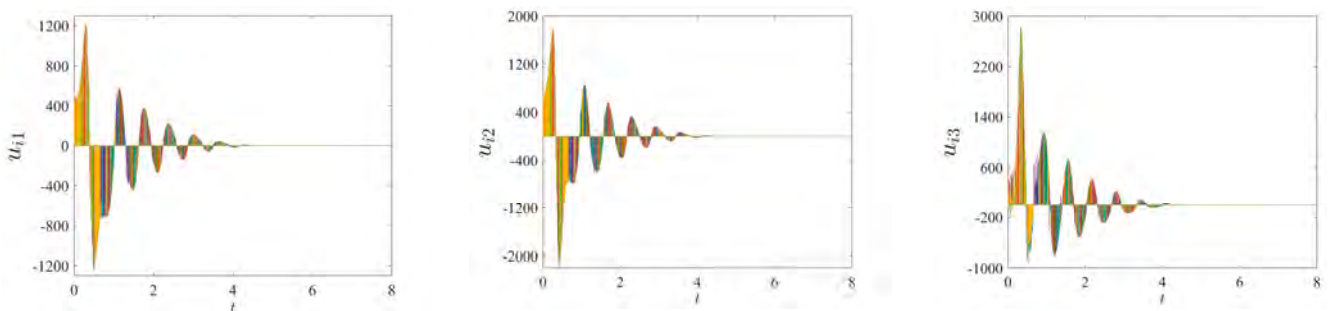


Figure 23. The update process of pinning controller $u_i(t)$ with time ($c_1 = c_2 = 0.1$).

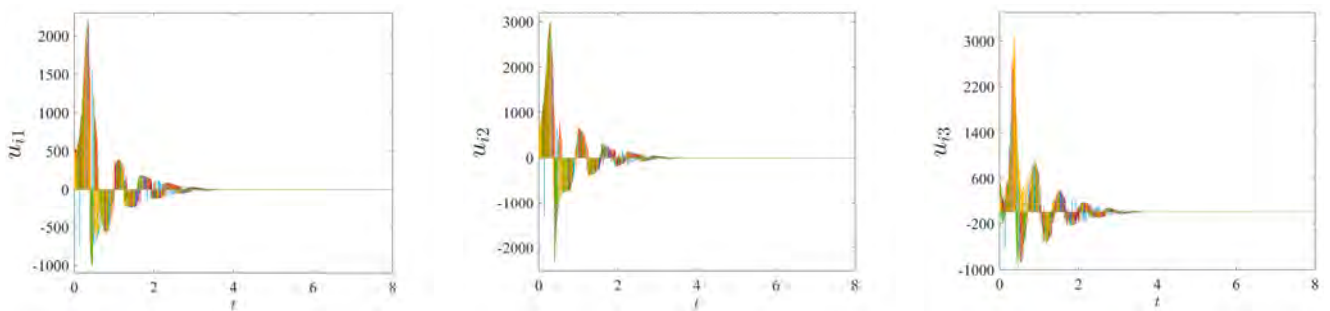


Figure 24. The update process of pinning controller $u_i(t)$ with time ($c_1 = c_2 = 0.001$).

Example 6. In this example, a multi-weight Markovian switching complex network model simulation with 100 nodes was performed using the event-triggered control strategy, and the coupling strengths of the networks were $c_1 = c_2 = 10$, $c_1 = c_2 = 1$, and $c_1 = c_2 = 0.4$, respectively. According to the established event-triggered function to update the controller at all synchronization times, and the three nodes of the network are selected as controlled nodes,

$$i.e., u_i(t) = \left(\overbrace{u_1(t), u_2(t), u_3(t)}^3, \overbrace{0, 0, \dots, 0}^{100-3} \right).$$

The control parameter ξ of the trigger function (31) is taken as $\xi = 0.7$; $\Xi(1) = \left(\overbrace{90, 72, 88}^3, \overbrace{0, 0, \dots, 0}^{100-3} \right)$, $\Xi(2) = \left(\overbrace{101, 83, 98}^3, \overbrace{0, 0, \dots, 0}^{100-3} \right)$. According to (34), we can get $t^* \leq 9.3369$ by simple calculation.

The network synchronization error curves and the event-triggered controller update process for different coupling strengths $c_1 = c_2 = 10$, $c_1 = c_2 = 1$ and $c_1 = c_2 = 0.4$ are given by Figures 25–30, respectively. Synchronization of the Markovian switching network can be achieved at $t \approx 0.1$ when the coupling strength $c_1 = c_2 = 10$, at $t \approx 1.2$ when the coupling strength $c_1 = c_2 = 1$, at $t \approx 5$ when the coupling strength $c_1 = c_2 = 0.4$. When the coupling strength of the network is very weak (less than 0.1 in Example 6), the Markovian complex network will no longer be synchronized under the event-triggered control strategy. This again validates the conclusion obtained in Example 3. Based on the event-triggered control

strategy, the synchronization time of the network gradually increases as the coupling strength of the network decreases, and the event-triggered controller is also step-varying.

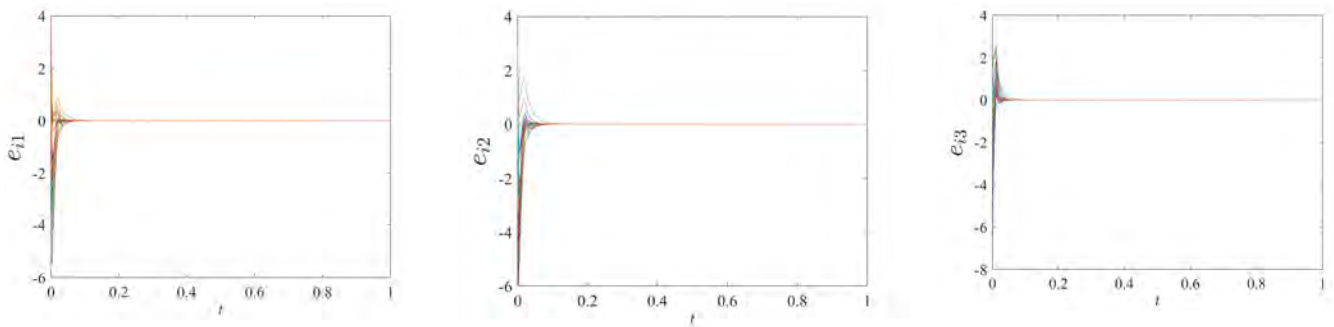


Figure 25. The synchronization error $e_i(t)$ of the network ($c_1 = c_2 = 10$).

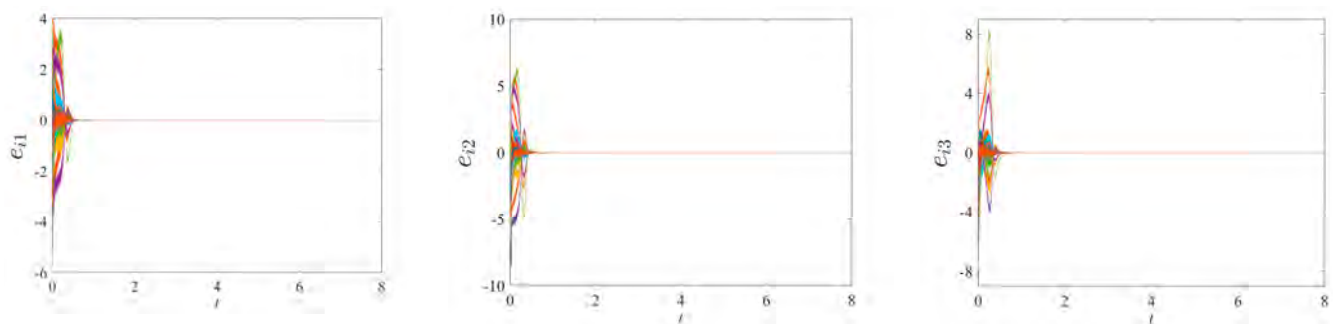


Figure 26. The synchronization error $e_i(t)$ of the network ($c_1 = c_2 = 1$).

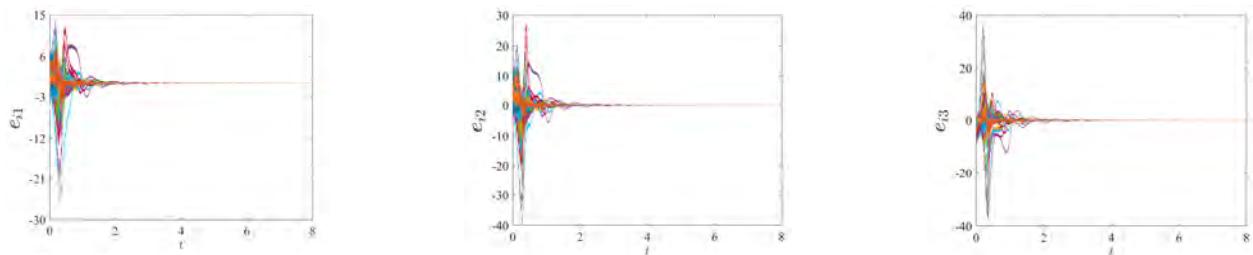


Figure 27. The synchronization error $e_i(t)$ of the network ($c_1 = c_2 = 0.4$).

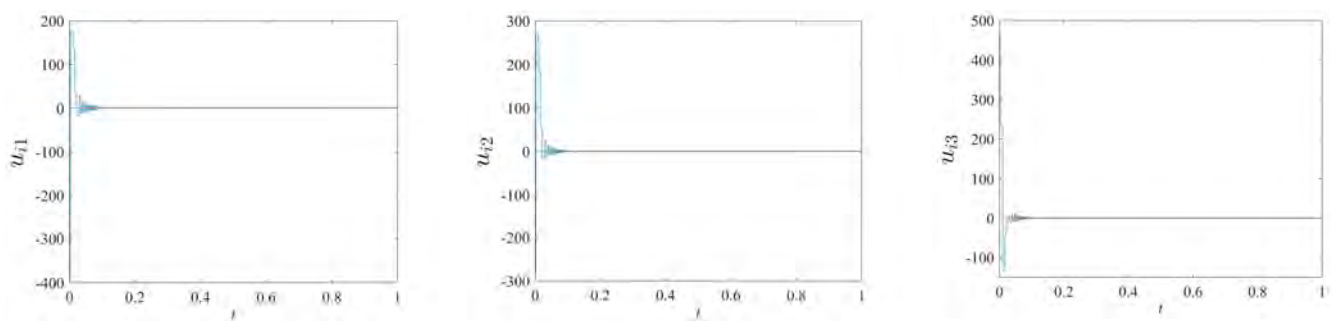


Figure 28. The update process of event-triggered controller $u_i(t)$ with time ($c_1 = c_2 = 10$).

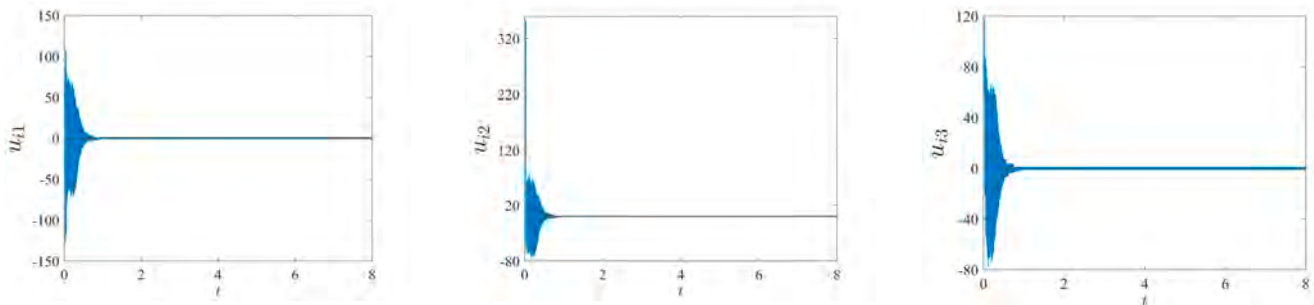


Figure 29. The update process of event-triggered controller $u_i(t)$ with time ($c_1 = c_2 = 1$).

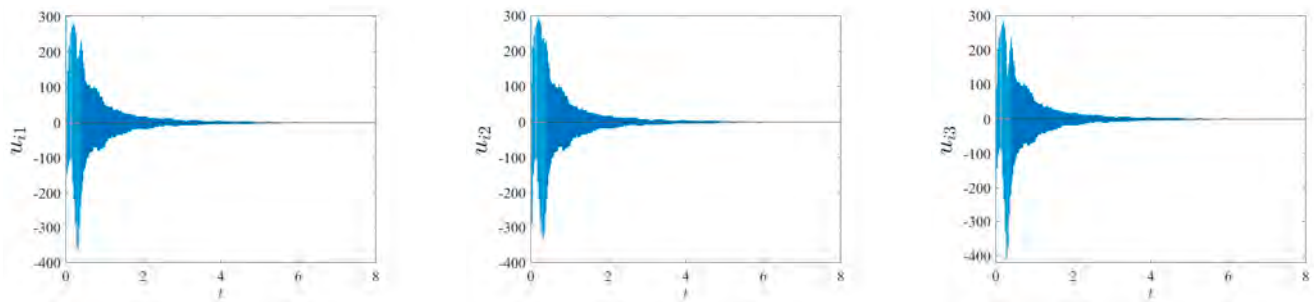


Figure 30. The update process of event-triggered controller $u_i(t)$ with time ($c_1 = c_2 = 0.4$).

Table 2 shows the comparison of the synchronization time of the two control strategies in Example 4 (100-nodes network) with different coupling strengths.

Table 2. Comparison of the synchronization time of two control strategies in Example 4.

Control Strategy	Coupling Strength	Synchronization Time
Optimal node selection	$(c_1 = c_2 = 10)$	$t \approx 4$
Event trigger control	$(c_1 = c_2 = 10)$	$t \approx 0.1$
Optimal node selection	$(c_1 = c_2 = 1)$	$t \approx 4$
Event trigger control	$(c_1 = c_2 = 1)$	$t \approx 1.2$
Optimal node selection	$(c_1 = c_2 = 0.1)$	$t \approx 4$
Event trigger control	$(c_1 = c_2 = 0.1)$	/
Event trigger control	$(c_1 = c_2 = 0.4)$	$t \approx 5$
Optimal node selection	$(c_1 = c_2 = 0.01)$	$t \approx 4$
Event trigger control	$(c_1 = c_2 = 0.01)$	/

The conclusions obtained in Example 1 can be verified again by analyzing the simulation results of Examples 2 and 3. When the coupling strength is large enough ($c_1 = c_2 = 10, 1$), the event-triggered control can achieve the synchronization faster. When the coupling strength gradually decreases ($c_1 = c_2 = 0.1, 0.001$), the Markovian complex network will no longer be able to achieve synchronization under the event-triggered control strategy, and the optimal node selection strategy can achieve the synchronization faster.

In addition to the above conclusions, by comparing Examples 1 and 4, it can be seen that as the number of network nodes continues to increase, the synchronization time of the network also increases under the optimal node selection strategy, and the time to achieve network synchronization under the proposed event-triggered control strategy will not change significantly as the number of network nodes increases.

6. Conclusions

This paper focuses on the analysis of low energy synchronization of Markovian switching complex networks through multiple perspectives. Analysis and discussion is based on the two control strategies of optimal node selection and event-triggered control.

- (1) Considering that the Markovian switching process will change the dynamic of the complex network, the optimal node selection strategy based on network node importance measurement is improved, and a controller with a simpler structure is designed, which can quickly achieve low energy synchronization of the complex network.
- (2) Considering the control cost problem caused by the large amount of information transfer between networks, a trigger function is designed that can eliminate invalid information intersection and transmission between networks based on the event-triggered control strategy, so as to achieve low energy synchronization of Markovian switching complex networks.
- (3) Based on the above two control strategies, important conclusions have been obtained through comparative simulation, which indicate that in order to optimally achieve synchronization control under low energy cost mechanism, a control strategy with faster synchronization speed and fewer control nodes is better.

I. Compared with event-triggered control strategy, the optimal node selection strategy can control less nodes (only one control node in Examples 2 and 5) to achieve network synchronization, which can further reduce the control cost of the network.

II. With the continuous increase of the network, the network synchronization time under the optimal node selection strategy has also increased. However, under the event-triggered control strategy, the time to achieve network synchronization will not change significantly with the growth of the network, but slightly more control nodes (three control nodes in Examples 5 and 6) are required compared to the optimal node selection strategy.

III. When the network coupling strength is large enough, the event-triggered control strategy can achieve synchronization faster. When the coupling strength of the network is very weak, the Markovian complex network can achieve synchronization faster under the optimal node selection strategy, and it will no longer be synchronized under the event-triggered control strategy.

Author Contributions: Conceptualization, Q.X.; methodology, Q.X.; software, Q.X.; validation, Q.X. and H.X.; formal analysis, Q.X., H.X., Z.W. and J.D.; investigation, Q.X., Z.W. and J.D.; data curation, Q.X., H.X., Z.W. and J.D.; writing—original draft preparation, Q.X. and H.X.; writing—review and editing, Q.X. and H.X. All authors have read and agreed to the published version of the manuscript.

Funding: This research was funded by National Nature Science Foundation of China (grant number 52009106).

Data Availability Statement: The data used to support the findings of this study are available from the corresponding author upon request.

Conflicts of Interest: The authors declare no conflict of interest.

References

1. Liu, X. Synchronization and Control for Multiweighted and Directed Complex Networks. *IEEE Trans. Neural Networks Learn. Syst.* **2023**, *34*, 3226–3233. [[CrossRef](#)] [[PubMed](#)]
2. Bao, Y.; Thesma, V.; Kelkar, A.; Velni, J.M. Physics-guided and Energy-based Learning of Interconnected Systems: From Lagrangian to Port-Hamiltonian Systems. In Proceedings of the 2022 IEEE 61st Conference on Decision and Control (CDC), Cancun, Mexico, 6–9 December 2022; pp. 2815–2820.
3. Hu, L.; Yang, Y.; Tang, Z.; He, Y.; Luo, X. FCAN-MOPSO: An Improved Fuzzy-Based Graph Clustering Algorithm for Complex Networks with Multiobjective Particle Swarm Optimization. *IEEE Trans. Fuzzy Syst.* **2023**, *31*, 3470–3484. [[CrossRef](#)]
4. Barabási, A.-L.; Albert, R. Emergence of Scaling in Random Networks. *Science* **1999**, *286*, 509–512. [[CrossRef](#)] [[PubMed](#)]
5. Cai, J.; Feng, J.; Wang, J.; Zhao, Y. Stochastic Synchronization of Semi-Markovian Switching Cyber-Physical Impulsive Complex Networks via Dynamic Event-Triggered SMC. *IEEE J. Emerg. Sel. Top. Circuits Syst.* **2023**, *13*, 752–766. [[CrossRef](#)]
6. Liang, K.; He, W.; Xu, J.; Qian, F. Impulsive Effects on Synchronization of Singularly Perturbed Complex Networks with Semi-Markov Jump Topologies. *IEEE Trans. Syst. Man Cybern. Syst.* **2022**, *52*, 3163–3173. [[CrossRef](#)]
7. Zhang, R.; Song, X.; Zhang, Y.; Song, S. Dissipative sampled-data synchronization for spatiotemporal complex dynamical networks with semi-Markovian switching topologies. *Neurocomputing* **2021**, *448*, 333–343. [[CrossRef](#)]
8. Wan, P.; Zeng, Z. Synchronization of Delayed Complex Networks on Time Scales via Aperiodically Intermittent Control Using Matrix-Based Convex Combination Method. *IEEE Trans. Neural Netw. Learn. Syst.* **2023**, *34*, 2938–2950. [[CrossRef](#)]

9. Xu, Y.; Gao, Q.; Xie, C.; Zhang, X.; Wu, X. Finite-Time Synchronization of Complex Networks with Privacy-Preserving. *IEEE Trans. Circuits Syst. II Express Briefs* **2023**, *70*, 4103–4107. [[CrossRef](#)]
10. Xia, Y.; Liu, X. Successive Lag Synchronization for Multilayer Complex Networks with Multiple Weights. *IEEE Trans. Circuits Syst. II Express Briefs* **2023**, *70*, 3514–3518. [[CrossRef](#)]
11. Wu, X.; Ai, Q.; Wang, Y. Adaptive and Exponential Synchronization of Uncertain Fractional-Order T-S Fuzzy Complex Networks with Coupling Time-Varying Delays via Pinning Control Strategy. *IEEE Access* **2021**, *9*, 2007–2017. [[CrossRef](#)]
12. Feng, J.; Cheng, K.; Wang, J.; Deng, J.; Zhao, Y. Pinning synchronization for delayed coupling complex dynamical networks with incomplete transition rates Markovian jump. *Neurocomputing* **2021**, *434*, 239–248. [[CrossRef](#)]
13. Ding, S.; Wang, Z.; Xie, X. Dynamic Periodic Event-Triggered Synchronization of Complex Networks: The Discrete-Time Scenario. *IEEE Trans. Cybern.* **2023**, *53*, 6571–6576. [[CrossRef](#)] [[PubMed](#)]
14. Liang, Y.; Deng, Y.; Zhang, C. Outer Synchronization of Two Multi-Layer Dynamical Complex Networks with Intermittent Pinning Control. *Mathematics* **2023**, *11*, 3543. [[CrossRef](#)]
15. Peng, H.; Huang, J.; Zhao, Z.; Wang, H.; Shi, P. H_∞ Pinning Synchronization Control for Markovian Intermittent Time-Varying Coupled Neural Networks Under Multiplicative Noises. *IEEE Trans. Circuits Syst. I Regul. Pap.* **2023**, *70*, 3712–3722. [[CrossRef](#)]
16. Liu, L.; Zhou, W.; Huang, C. Finite/Prescribed-Time Cluster Synchronization of Complex Dynamical Networks with Multi-proportional Delays and Asynchronous Switching. *IEEE Trans. Syst. Man Cybern. Syst.* **2023**, *53*, 3683–3694. [[CrossRef](#)]
17. Jafarizadeh, S. Pinning Control of Dynamical Networks with Optimal Convergence Rate. *IEEE Trans. Syst. Man Cybern. Syst.* **2022**, *52*, 7160–7172. [[CrossRef](#)]
18. Cao, Z.; Li, C.; He, Z.; Zhang, X.; You, L. Synchronization of Coupled Stochastic Reaction-Diffusion Neural Networks with Multiple Weights and Delays via Pinning Impulsive Control. *IEEE Trans. Netw. Sci. Eng.* **2022**, *9*, 820–833. [[CrossRef](#)]
19. Liang, H.; Chang, Z.; Ahn, C.K. Hybrid Event-Triggered Intermittent Control for Nonlinear Multi-Agent Systems. *IEEE Trans. Netw. Sci. Eng.* **2023**, *10*, 1975–1984. [[CrossRef](#)]
20. Gong, C.; Zhu, G.; Shi, P. Adaptive Event-Triggered and Double-Quantized Consensus of Leader-Follower Multiagent Systems with Semi-Markovian Jump Parameters. *IEEE Trans. Syst. Man, Cybern. Syst.* **2021**, *51*, 5867–5879. [[CrossRef](#)]
21. Chen, H.; Shi, P.; Lim, C.-C. Synchronization Control for Neutral Stochastic Delay Markov Networks via Single Pinning Impulsive Strategy. *IEEE Trans. Syst. Man Cybern. Syst.* **2020**, *50*, 5406–5419. [[CrossRef](#)]
22. Xie, Q.; Guo, D.; Wang, T.; Yang, X. Finite-time synchronization and identification of the Markovian switching delayed network with multiple weights. *IET Control. Theory Appl.* **2021**, *15*, 1571–1587. [[CrossRef](#)]
23. Yuan, C.; Mao, X. Robust stability and controllability of stochastic differential delay equations with Markovian switching. *Automatica* **2004**, *40*, 343–354. [[CrossRef](#)]

Disclaimer/Publisher’s Note: The statements, opinions and data contained in all publications are solely those of the individual author(s) and contributor(s) and not of MDPI and/or the editor(s). MDPI and/or the editor(s) disclaim responsibility for any injury to people or property resulting from any ideas, methods, instructions or products referred to in the content.